Cruise Report
KN180-2
RV KNORR

Bermuda – Woods Hole
Nov 14th Dec 17th 2004

Kane Megamullion
2004

NSF Grant OCE-0118445

Maurice Tivey, Brian Tucholke, Henry Dick,
and Shipboard Science, JASON-2, and ABE Technical Teams

Woods Hole Oceanographic Institution
Woods Hole, MA 02543, USA

Cruise Report

R/V Knorr
KN180-2

Kane Megamullion 2004

Magnetic and Structural Studies of a Lower Crustal Exposure of Ocean Lithosphere: Kane Megamullion, Mid-Atlantic Ridge 23°30'N.

NSF Grant OCE-0118445

St. Georges, Bermuda to Woods Hole, MA USA
November 14th 2004 to December 17th 2004

Maurice Tivey, Brian Tucholke, Henry Dick,
and Shipboard Science, JASON-2, and ABE Technical Teams

Woods Hole Oceanographic Institution
Woods Hole, MA 02543, USA

R/V Knorr KN180-2
Personnel List

Science Passengers

1) Dr. Maurice Tivey	WHOI	mtivey@whoi.edu	Chf. Scientist
2) Dr. Brian Tucholke	WHOI	btucholke@whoi.edu	Co-Chf. Scientist
3) Dr. Henry Dick	WHOI	hdick@whoi.edu	Co-Chf. Scientist
4) Dr. Steve Swift	WHOI	sswift@whoi.edu	Data Manager
5) Eben Franks	WHOI	efranks@whoi.edu	Dredge Master
6) Clare Williams	WHOI	clare@whoi.edu	Watchstander
7) Jessica Warren	WHOI	jmwarren@whoi.edu	Watchstander
8) Dylan Malynn	UMass	dmalynn@student.umass.edu	Dredge Asst.
9) Dr. Mike Cheadle	UWy	cheadle@uwyo.edu	Guest Scientist
10) Josh Schwartz	UWy	schwartz@uwyo.edu	Watchstander
11) Bridget Diefenbach	U Idaho	dief5183@uidaho.edu	Watchstander
12) Kay Achenbach	UWy	kay@uwyo.edu	Watchstander
13) Dr. Al Bradley	WHOI ABE	abradley@whoi.edu	ABE
14) Dr. Dana Yoerger	WHOI ABE	dyoerger@whoi.edu	ABE
15) Rod Catanach	WHOI ABE	rcatanach@whoi.edu	ABE
16) Matt Heintz	WHOI DSL	mheintz@whoi.edu	Pilot ExpLdr
17) Jim Varnum	WHOI DSL	jimv@drizzle.com	Pilot
18) Phil Forte	WHOI DSL	pforte@whoi.edu	Pilot
19) Bob Waters	WHOI DSL	b_waters@charter.net	Eng
20) Bob Elder	WHOI DSL	relder@whoi.edu	Eng
21) Brian Bingham	WHOI DSL	bbingham@whoi.edu	Nav
22) Will Handley	WHOI DSL	handleys@compuserve.com	Nav
22) Dara Scott	WHOI DSL	dara_scott@hotmail.com	Nav
23) Casey Agee	WHOI DSL	Kcagee1@cs.com	Eng
24) Tom Bolmer	WHOI-DSL	tbolmer@whoi.edu	Data

Ship's Crew

A. D. Colburn	Captain
Kent Sheasley	1st Mate
Dee Emrich	2nd Mate
Derek Bergeron	3rd Mate
Peter Liarikos	Bosun
Kevin Butler	AB
William Dunn	AB
Edward Graham	AB
Bankole Salami	OS
Lorna Allison	OS
Steve Walsh	Chf. Engineer
Patrick Mone	1st Engineer
Wayne Silvia	2nd Engineer
Piotr Marczak	3rd Engineer
Thidiane Kanoute	Electrician
Andrew Gillen	Oiler
Allen Farrington	Oiler
Russell Adams	Oiler
Mirth Miller	Chf Steward
Brian O'Nuallain	Cook
Jim Brennan	Mess Attendant
Robert Laird	SSSG
Amy Simoneau	SSSG
Jeff Perkins	Comm/ET

Table of Contents

Appendices

Figure List

Acknowledgments

We thank the operational teams for Jason-2 and ABE for their efforts in making KN180-02 a tremendously successful cruise. We thank Matt Heintz for his leadership of the Jason team and Dana Yoerger and Al Bradley for the ABE team. We also thank Captain A.D. Colburn, along with his officers and crew of the RV Knorr for their help and operational knowledge in making this an enjoyable and rewarding experience. We also thank the science team and specifically Dr. Mike Cheadle for leading the way in the rock descriptions. It was a small science party and so everyone contributed significantly to the ultimate success of the program.

Magnetic and Structural Studies of a Lower Crustal Exposure of Ocean Lithosphere: Kane Megamullion, Mid-Atlantic Ridge 23°30'N.

CRUISE OBJECTIVES

The objective of the cruise is to investigate three basic questions about the structure and evolution of slow-spreading ocean crust, and at the same time to obtain site-survey data for a proposed Integrated Ocean Drilling Project (IODP) program. The cruise focuses on the Kane megamullion or oceanic core-complex located at 23º 30'N, 45º 20'W on the western flank of the Mid-Atlantic Ridge at Kane (MARK) area (see Figures 1, 2 and 3). The Kane megamullion is interpreted to be the exhumed footwall of a long-lived (~1.2 m.y.) normal "detachment" fault near Kane Fracture Zone (F.Z.) on 2.7 million year-old crust. This exhumation appears to have exposed an upper-mantle section of lithosphere and a deep-crustal section that is readily accessible to survey, sampling, and eventual drilling. The fault surface is characterized by smooth topography interrupted by a distinct series of linear ridges, corrugations, or mullions that are oriented parallel to the spreading flow-line direction and perpendicular to the spreading axis and abyssal hill lineations. The Kane megamullion area also shows well defined magnetic lineations of Chron 2A without any major disruptions, implying the presence of coherently magnetized source rocks (Fig. 3). The three primary scientific questions addressed with this program are:

- How are magnetization and the polarity-reversal history of Earth's magnetic field recorded at mid-crustal and deeper levels?

- What conditions of magmatism at the rift axis attend formation of megamullions, and what are the resulting composition and intrusive relations at mid-crustal and deeper levels?

- What are the nature of strain accommodation and evolution of strain localization in the shear zone of a major normal fault in ocean crust?

The field program described here (KN180-2) used 1) the ROV Jason-2 (hereafter Jason) for sampling and imaging of the fault scarps that cross-cut the megamullion surface, 2) the autonomous underwater vehicle ABE for magnetic, bathymetric, photo and chirp sonar mapping, and 3) rock dredging to determine a broad, multi-kilometer-scale lithologic and petrologic context of the study area. We also collected SeaBeam 2100 swath bathymetry, 3.5 khz profiles and sea surface magnetic data at the beginning of the program and then later in the program.

Background : Megamullions

Megamullions or oceanic core complexes have been identified at more than two dozen locations on the Mid-Atlantic Ridge (Tucholke et al., 1996; Cann et al., 1997; Tucholke et al., 1998b; Casey et al., 1998). They also occur on the Southeast Indian Ridge in the Australia-Antarctic Discordance (Sempéré et al., 1998), and on the Southwest Indian Ridge (Mitchell et al., 1998; Searle et al., 1998; Fujimoto et al., 1998; Dick et al., 1999). They occur at spreading ridges characterized by limited magma supply, regardless of spreading rate, and they form predominantly in "inside-corner" (IC) tectonic settings adjacent to ridge-axis discontinuities. Megamullions appear as domes or plateaus up to tens of kilometers in diameter, and they have corrugated surfaces with elongated lineations or mullions oriented parallel to the spreading direction. They also exhibit residual mantle Bouguer gravity (RMBA) anomalies that are up to 20-25 mGal higher than over adjacent normal lithosphere, and they consistently expose gabbros and serpentinized peridotites (see Tucholke et al. (1998b) for a synthesis of megamullion characteristics). These observations suggest that megamullions are developed by fault extension that exposes deep structural levels of ocean crust and upper mantle.

Megamullions have been cited as oceanic analogs of continental metamorphic core complexes because of their similar scale, morphology, and apparent mode of formation (e.g., Cann et al., 1997; Tucholke et al., 1998b; Karson, 1999). However, megamullions in many ways are simpler. Compared to continental core complexes, for example, exposure of megamullion domes is typically complete and is unaffected by major erosion; the host rocks have limited compositional variation and they have not suffered previous orogenesis; the kinematic framework of megamullion formation is well constrained; and the geologic setting places narrow strictures on interpretations of magnetization.

Background : Geologic Setting of Kane Megamullion Area

The Kane megamullion area is well surveyed with surface-ship multibeam bathymetry, gravity, and magnetics (Pockalny et al., 1988; Gente et al., 1995; Morris et al., 1989; Fujimoto et al., 1996; Maia and Gente, 1998; Schulz et al., 1988; Pockalny et al., 1995). RMBA gravity is elevated (~20-28 mGal) over most of the Kane megamullion and the adjacent fracture-zone wall, suggesting densities greater than in a normal crustal section. The gravity high is located between the breakaway and the center of the megamullion dome, which is typical of the majority of known megamullions (Tucholke et al., 1998b). Prior to this cruise, sampling and on-bottom work concentrated on the present inside-corner high east of the Kane megamullion (Dick et al abstract, Karson et al., 1992; Auzende et al., 1994) and the Kane transform wall that forms the north edge of the megamullion (Auzende et al., 1994). A deep-tow sidescan survey also examined the fracture zone wall and northernmost edge of the megamullion up to 40 km west of the ridge-transform intersection (Karson et al., 1992; Gao et al., 1998). The observations where the megamullion abuts Kane F.Z. show that the detachment fault has exhumed gabbros and serpentinized peridotites, consistent with elevated gravity values, although they also show structural complications related to fracture-zone tectonics (e.g., high-angle dip-slip and possibly strike-slip faults).

Magnetic anomalies over the Kane megamullion show no significant change in character from the adjacent, normal crust. This is puzzling because the primary location of crustal magnetization classically has been considered to be the volcanic layer (e.g., Talwani et al., 1971; Harrison, 1987), yet the detachment model and limited previous seafloor observations predict that a megamullion is exhumed sub-volcanic crust and upper mantle. A magnetized gabbro section may explain the presence of magnetic anomalies over Kane megamullion. A recent study of crustal magnetization on the west flank of the MAR (Tivey and Tucholke, 1998) suggests that most magnetization in the volcanic layer is attenuated immediately off-axis and that lower crust and upper-mantle serpentinites may be a major contributor to the ridge-flank magnetic anomaly signal at slow-spreading ridges. Oceanic gabbros can have significant stable remanent magnetization, although it is generally less intense than in basalts (Kent et al., 1978; Pariso and Johnson, 1993b; Pariso and Johnson, 1993a; Kikawa and Ozawa, 1992). Reversely magnetized gabbros have been drilled at Atlantis Bank megamullion on the Southwest Indian Ridge, and a minor reversal boundary that may correlate with the geomagnetic time scale has been identified (Allerton and Tivey, 1998).

Two major domal surfaces were investigated in detail during this cruise. The northern dome (here called Babel Dome) is a relatively small feature that extends 12km long flowlines adjacent to the Kane FZ. The larger southern domes (Cain and Abel Domes) are ~25 km long with a 400 m high cross-cutting scarp that parallels isochrons. The detachment fault over the surface of the Kane megamullion extends ~35 km N-S along strike, encompassing roughly 70% of the enclosing spreading segment from Kane F.Z. southward toward a non-transform discontinuity. In the dip direction, it reaches ~23 km from the breakaway (fault initiation) in ~3.4 Ma crust to fault termination ~1.2 m.y. later at the base of a hummocky ridge. The fault surface dips ~25° east towards the termination, but up to 10° west towards the breakaway in the west, thus forming a broad dome. The ridge east of the termination contacts the detachment surface in an isochron-parallel line that sinuously follows the mullions in the detachment surface. The ridge appears to be a remnant of the original hanging wall and is interpreted to have been stranded by an eastward ridge jump that caused the detachment fault to be abandoned during Chron 2n. Individual, large-amplitude (~0.4 km) mullion structures can be traced ~E-W for more than 20 km from near the interpreted breakaway to the fault termination, indicating that they were all formed along one detachment fault.

The detachment surface is interrupted by high-angle faults that may have formed in response to bending stresses during footwall rollover (Manning and Bartley, 1994). Most notably, in the middle of the megamullion in ~2.7 Ma crust, a steep scarp offsets the detachment surface by 250 to 550 m. This is the largest-offset scarp in any known megamullion, and it provides the best available opportunity to access the interior of a megamullion without drilling. The ROV Jason dives focused on traversing this scarp face in two main areas with a thrid dive crossing over the fault surface of Cain dome and a fourth dive traversing a related high-angle fault to the southwest. The high-angle faults and surface of the megamullion dome were also studied using ABE and rock dredging.

Table 1 Magnetic chrons from Cande and Kent (1995).

Age (begin) M.y.	**Age (end) M.y.**	**Chron Number**	**Chron Name**
0.000	0.780	1n	Brunhes/Matuyama
0.990	1.070	1r.1n	Jaramillo
1.770	1.950	2n	Olduvai
2.140	2.150	2r.1n	Reunion
2.581	3.040	2An.1n	Matuyama/Gauss
3.110	3.220	2An.2n	
3.330	3.580	2An.3n	Gauss/Gilbert
4.180	4.290	3n.1n	Cochiti

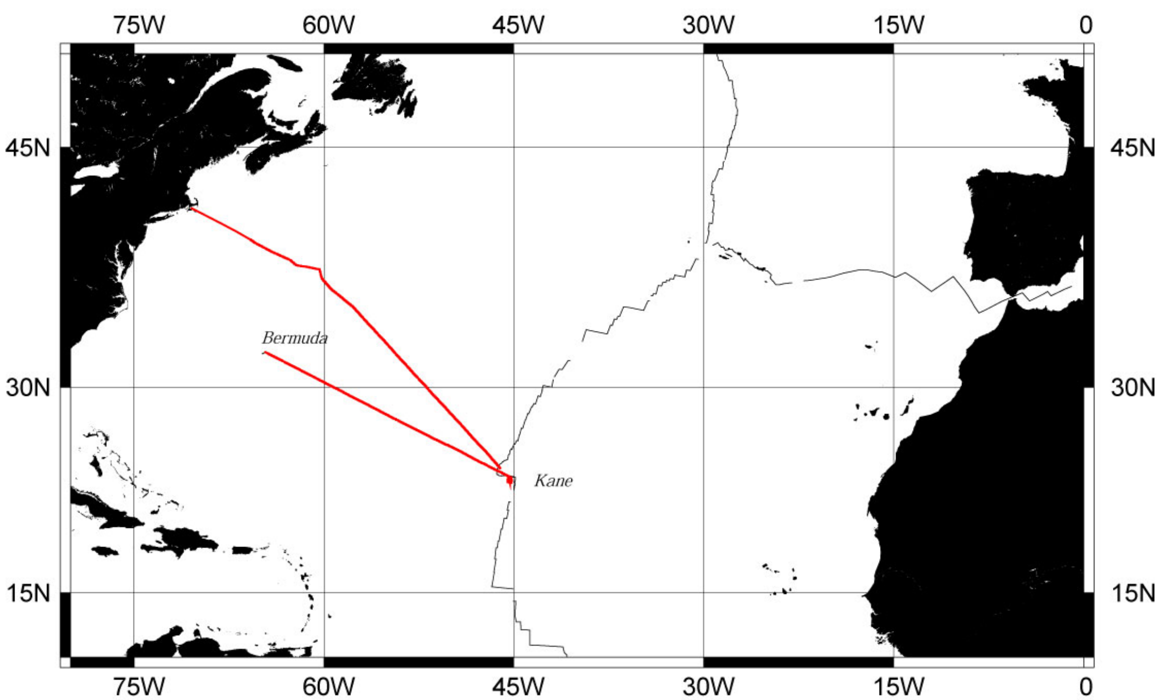

Figure 1. Location map and transit shiptrack of RV Knorr for research cruise KN180-2.

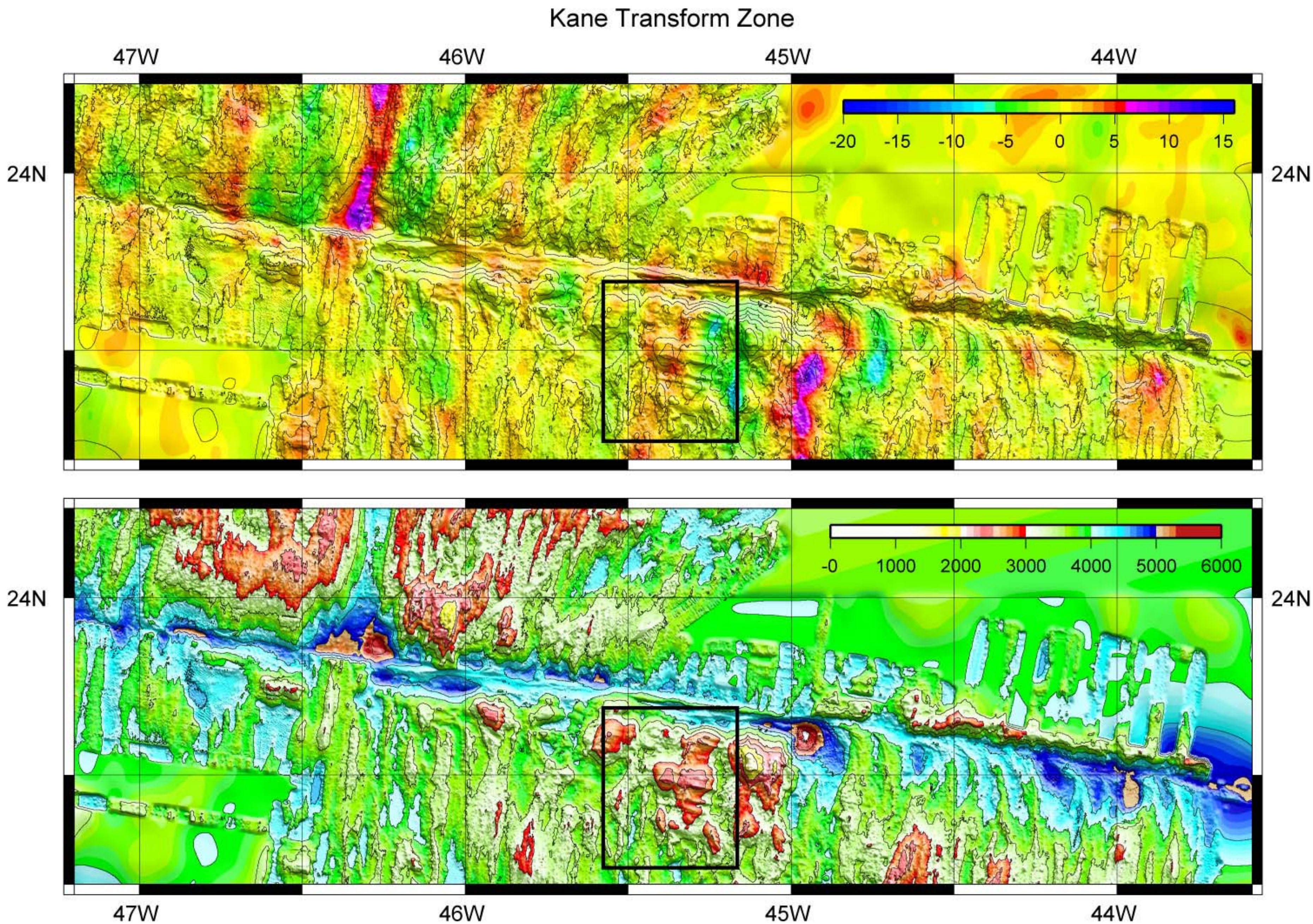

Figure 2. Kane transform zone showing the study area (bold box) in the bathymetry (bottom) and magnetization (top) in context with the surrounding terrain.

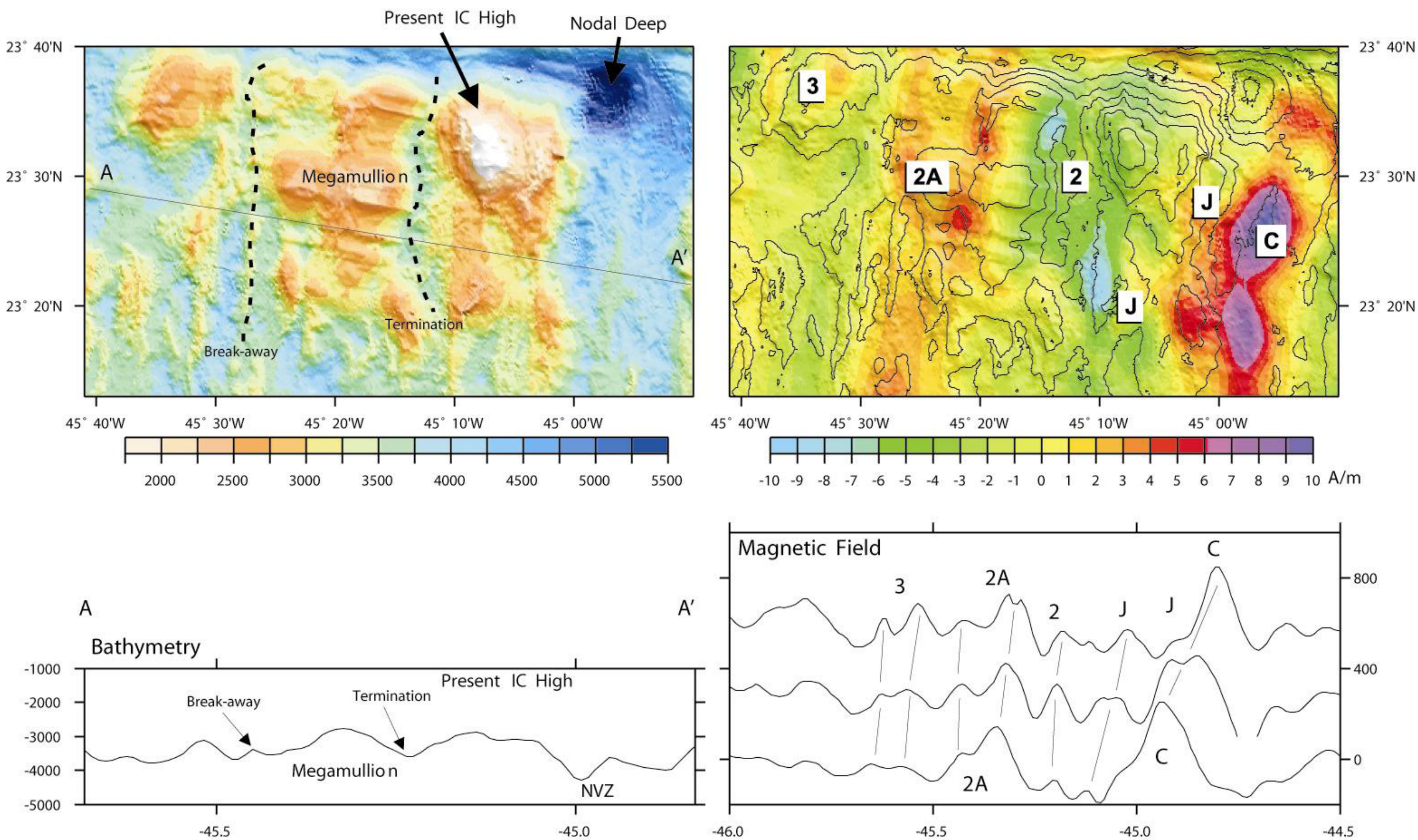

Figure 3. Top left is a shaded relief image (light from NW) of the megamullion detachment fault surface adjacent to Kane Transform formed at the inside corner of the ridge-transform intersection. The break-away zone of the detachment fault and it's termination are marked by dashed lines and are labeled. Top, right-hand figure shows computed crustal magnetization with identified magnetic anomalies that continue uninterrupted across the megamullion feature. Lower left figure taken along profile A-A' in bathymetry shows the relationship between the termination and break-away and the gently domed shape of the megamullion and detachment fault surface. NVZ indicates present day neovolcanic zone. Lower right figure shows identified magnetic anomaly chrons .

JULIAN DAY CALENDAR

Calendar	Julian Day
14-Nov-04	319
15-Nov-04	320
16-Nov-04	321
17-Nov-04	322
18-Nov-04	323
19-Nov-04	324
20-Nov-04	325
21-Nov-04	326
22-Nov-04	327
23-Nov-04	328
24-Nov-04	329
25-Nov-04	330
26-Nov-04	331
27-Nov-04	332
28-Nov-04	333
29-Nov-04	334
30-Nov-04	335
1-Dec-04	336
2-Dec-04	337
3-Dec-04	338
4-Dec-04	339
5-Dec-04	340
6-Dec-04	341
7-Dec-04	342
8-Dec-04	343
9-Dec-04	344
10-Dec-04	345
11-Dec-04	346
12-Dec-04	347
13-Dec-04	348
14-Dec-04	349
15-Dec-04	350
16-Dec-04	351
17-Dec-04	352

ROV JASON 2 -COMPONENTS

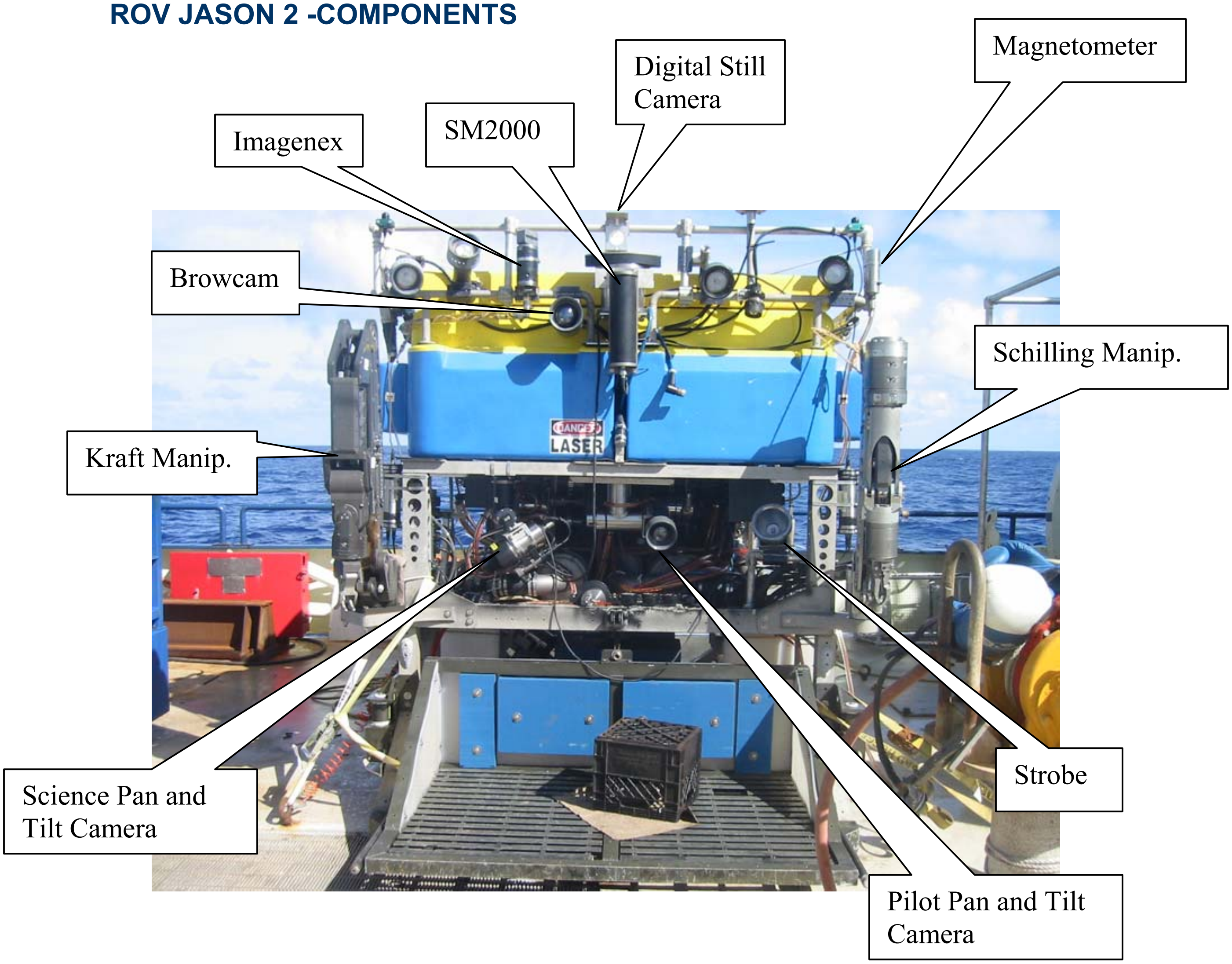

Figure 4. Jason-2 showing the major sonars, cameras and manipulators on the front of the vehicle. The Imagenex scanning sonar was used in an obstacle-avoidance mode and was not recorded. The SM2000 (Simrad 2000) was used in a forward looking mode for the first few dives and then moved to the rear of the vehicle looking down for dives 116 and 117. The digital still camera was borrowed from Dan Fornari and had to be downloaded after each dive. The three video channels recorded were the Brow-cam, Science Pan and Tilt and Pilot Pan and Tilt. The Brow video camera was fixed looking horizontal for dives 110 through 115 after which it was moved to look down at angle 47 degrees. The Science pan and tilt and Pilot pan and tilt were the two primary video cameras. A three-axis Honeywell HMR2300 magnetoresistor magnetometer was mounted on the top port side of Jason to measure magnetic fields. A redox potential (Eh) sensor was also provided by Dr. Ko-ichi Nakamura of the University of Tokyo in order to detect the possible presence of off-axis hydrothermal activity.

Figure 5. Aft view of Jason-2 showing the aft thrusters and doppler navigation systems. The 1200 khz Doppler had limited range and was supplanted by the 300 Khz Doppler system borrowed from Hanu Singh.

Figure 6. Medea Towed Vehicle is the cable junction box between the main armored cable and the umbilical tether to ROV Jason-2.

AUTONOMOUS BENTHIC EXPLORER (ABE)

Figure 7. The autonomous underwater vehicle ABE is a self-navigating vehicle that is programmed to follow a prescribed survey mission on the seafloor. ABE navigates by using an acoustic transponder net and a sophisticated seafloor avoidance algorithm. The primary sensor packages used in this study were the Simrad 2000 multibeam sonar (SM2000), magnetometer, digital still camera and a newly added sub-bottom chirp sonar. Note that for this cruise ABE had a depth limit of 3000 meters due to the depth rating of the SM2000 sonar.

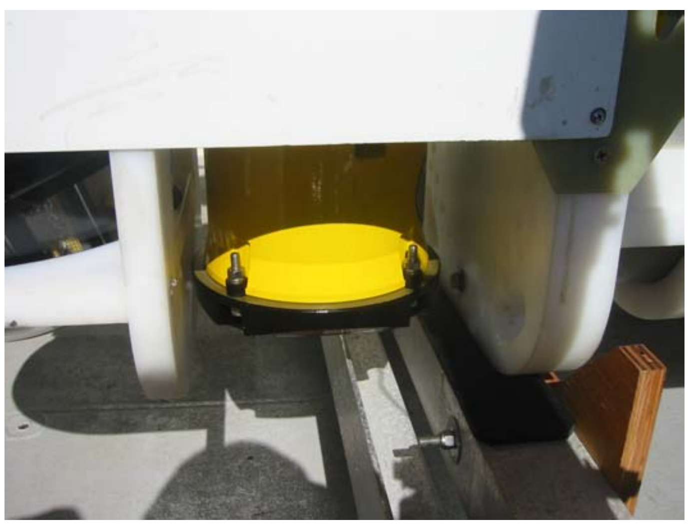

Figure 8. Photograph of the newly installed Edgetech chirp sonar system that was used to obtain sub-bottom data in order to determine sediment thickness in the study area.

SEA SURFACE MAGNETOMETER

Figure 9. Left shows towed magnetometer sensor. Right photo shows the cable spool.

The new WHOI “Geomag” sea surface magnetometer (left) was used for the first time on this cruise (KN180-2). The sensor is a new “Overhauser” type of nuclear precession type of magnetometer, which provides an absolute measurement of Earth’s total magnetic field with a precision of 0.1 nT. The sensor was towed 1000 feet behind the ship at a standard underway ship speed of 12 knots.

ECHOSOUNDING PROFILES

Echosounding profiles (3.5 and 12 kHz) in various formats were recorded throughout the cruise. The 12 kHz profiler was operated from Bermuda to the Kane megamullion study area and from the study area to Woods Hole; these data were recorded and provided on disk to the science party as ASCII files of depths every 1 minute along track. In the Kane study area, digital files of both 3.5 and 12 kHz data were recorded and were provided to the science party on disk. These files are in three formats: SEGY, binary files in .keb proprietary format, and ASCII depth files for each ping. The 3.5 kHz data are identified as LF files and the 12 kHz data are identified as HF files. Included on the data disk is the Knudsen software ‘postsurvey.exe’ that can be used to view the binary files and to extract images from them. The only paper records made during the cruise were 3.5 kHz profiles obtained in the Kane study area. These were provided to the Chief Scientist, and they will be archived in the WHOI Data Library and Archive together with other cruise data.

SEABEAM BATHYMETRY

The SeaBeam 2100 multibeam bathymetric system was operated throughout the cruise. In addition to underway data recorded during transit, the system was used to conduct two surveys. The first was a survey of Kane megamullion, which was made when we first arrived at the study area. These data provided bathymetry that improved upon the existing multibeam data from the RIDGE database, plus it provided beam-point amplitude information. The depth and amplitude data were essential for characterizing seafloor structural features and for assessing the presence or absence of significant sediment cover in areas where we wanted to dredge or run Jason transects.

The second multibeam survey was run over Hydrographer Canyon in the continental slope south of Georges Bank. This was a survey of opportunity, and it was conducted because we had about 19 extra hours of ship time available after having transited from the Kane area to the New England continental shelf at speeds better than had been predicted.

In addition to the above, we designed our ship track to cross over most of the New England Seamounts on our return leg from the Kane study area to Woods Hole. This was done at the request of Dr. Dan Scheirer who is studying the seamounts, and it did not add significantly to our transit time to Woods Hole.

All the SeaBeam data were recorded on disk and are archived at Woods Hole Oceanographic Institution. The data will be provided to NGDC after a one-year proprietary period.

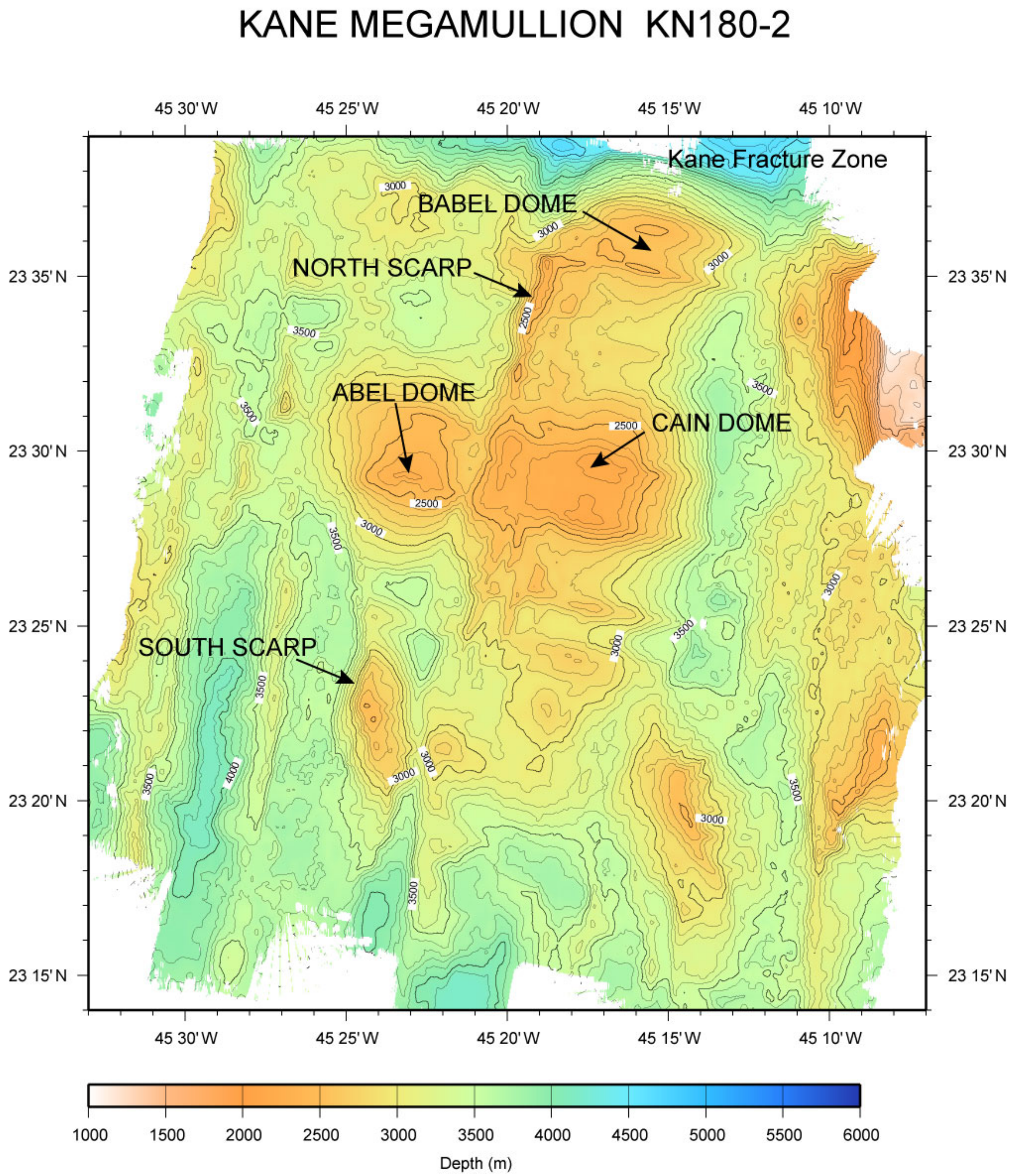

Figure 10. Seabeam map collected over the study area showing the two domal areas. Kane Fracture Zone borders the northern edge of the map.

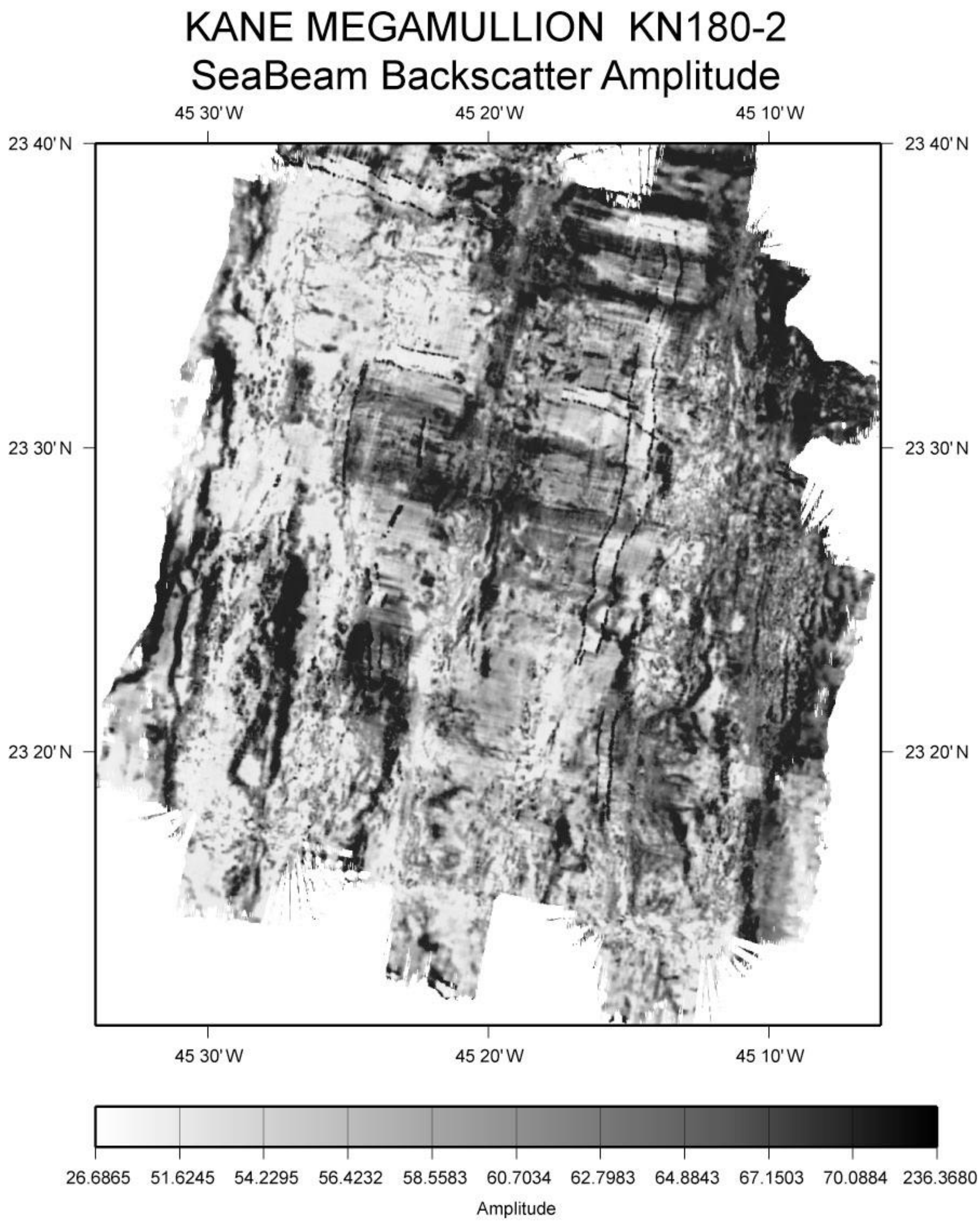

Figure 11. Seabeam backscatter amplitude map collected during the cruise over the study area.

UNDERWAY LOG

JD319 - Sun 14 November 2004

At 09:00 local time departed Penno's Wharf, St. Georges, Bermuda.
Local time was GMT+4 (Atlantic Standard Time)
Waypoint given to Bridge, 23° 35N 45° 20'W

JD320 - Mon 15 November 2004

06:00 (GMT) Began recording SeaBeam and 3.5 Khz reflection profiles.

JD321 - Tue 16 November 2004

In transit.

JD322 – Wed 17 November 2004

In transit. Deployed new Geomag sea surface magnetometer at 14:45. Experimented with logging the data. The sensor spits out a NMEA string of mag data but cannot get the GPS data string to be accepted by the Geomag data logging program. Tried to log it through the ship's Athena system, and that seems to work.

JD323 - Thu 18 November 2004

In transit. Did an XBT on approach to study site.
Began SeaBeam and sea surface magnetic survey of study area at 17:00 for an ~18 hour period.

JD324 - Fri 19 November 2004

End of Sea Beam and magnetic survey at 12:00.
Deployed first transponder net and surveyed them in (Net #1).
Proceeded to dredge target (K-1), Dredge station DR-1.

JD325 - Sat 20 November 2004

Launched ABE Dive 142
Proceeded to dredge target (K-3), Dredge station DR-2.
Proceeded to dredge target (K-5), Dredge station DR-3 (no recovery).
ABE recovered and on deck after a short dive.
Proceeded to dredge target (K-6), Dredge station DR-4.
Jason-2 launched, Dive 110 at 22:13.

JD326 - Sun 21 November 2004

04:20 Jason-2 back on deck. Oil leak in compensation system.
Proceeded to dredge target (K-7), Dredge station DR-5.
Proceeded to dredge target (K-9), Dredge station DR-6.
Proceeded to dredge target (K-13), Dredge station DR-7.
Jason-2 launched, Dive 111 at 18:53.

JD327 - Mon 22 November 2004

End of Jason-2 Dive 111, 06:46
Redeployed transponder net for ABE run over Babel Dome and surveyed in the transponders (Net #2).
Proceeded to dredge target (K-14) but ship's nav began to drop out: both differential C-Nav and P-code GPS were flaky.
Proceeded to dredge target (K-15) Dredge station DR-8.
Began preparing for ABE dive but dive is delayed because of a problem with the vehicle.
Proceeded to dredge target (K-14), Dredge station DR-9.

JD328 - Tue 23 November 2004

Launch ABE dive 143 for Babel Dome run.
ABE is on bottom and running so proceeded to dredge target (K-8), Dredge station DR-10.
Proceeded to dredge target (K-20), Dredge station DR-11.
Proceeded to dredge target (K-23), Dredge station DR-12.
ABE recovered at 17:30 and on deck.
Released all four transponders from Net#2 and redeployed at southern dome site (Cain and Abel Domes).

JD329 – Wed 24 November 2004

Proceeded to dredge target (K-21) Dredge station DR-13.
Preparing for ABE dive 144 but it had problems again and so we went off to do a dredge. Proceeded to dredge target (K-17) Dredge station DR-14.
ABE Dive 144 launched at 18:36. Waited for ABE to reach the bottom.
By 21:32 we proceeded to dredge target (K-18) Dredge station DR-15.

JD330 - Thu 25 November 2004 Thanksgiving Day

Proceeded to dredge target (K-19), Dredge station DR-16. Afterwards we waited for ABE to finish its survey and return to the ship. By 14:08 ABE was on deck. We then prepared to launch JASON.
JASON Dive 112 launched at 15:04 on west-facing fault scarp face of Cain Dome.

JD331 - Fri 26 November 2004

JASON Dive 112 continued. We did an elevator run at 08:00. Elevator was on deck by 09:56.

JD332 - Sat 27 November 2004

JASON Dive 112 continued.

JD333 - Sun 28 November 2004

Recovered JASON at 20:30. End of JASON Dive 112. Moved ship to the next ABE launch point. We launched ABE Dive 145 at 16:35. Tracked ABE to the bottom before moving off to do the next dredge.

JD334 - Mon 29 November 2004

Proceeded to dredge target (K-28), Dredge DR 17.
02:59 ABE may have had problems so we drove over to listen to it. ABE seemed okay so we moved to dredge target (K-12), Dredge DR-18.
Proceeded to dredge target (K-19), Dredge station DR-19.
At 14:00 we began a short SeaBeam and magnetics survey prior to ABE recovery. We suspended the survey after crossing 45° 14'W to go and pick up ABE. We initially were in ABE search mode and were not sure where it was.
ABE was found and recovered at 16:53. It had just surfaced.
JASON Dive 113 was launched at 19:39 on east-facing side of Abel Dome.

JD335 - Tue 30 November 2004

JASON Dive 113 continued on east-facing side of Abel Dome.

JD336 - Wed 1 December 2004

JASON had a hydraulic problem and had to abandon the dive. Compensation fluid in main transformer was low in oil. Recovered JASON at 06:00.
Proceeded to dredge target (K-35), Dredge station DR-20.
Proceeded to dredge target (K-33), Dredge station DR-21.
Proceeded to dredge target (K-24), Dredge station DR-22.
JASON was fixed and Dive 114 was launched at 22:41.
JASON Dive 114 was located again over the east-facing side of Abel Dome.

JD337 - Thu 2 December 2004

Operations had been going well until JASON had a problem with its tether. While waiting for an elevator and getting rid of some warps and kinks in the tether the pilot yanked the tether and lost telemetry. JASON was brought up and was on deck at 16:54. End of JASON Dive 114.
Released three transponders (G,H,I) and redeployed all three in a line along the Cain dome for a magnetics run using ABE.

JD338 – Fri 3 December 2004

Finished transponder surveying and geared up for an ABE dive. ABE launched at 02:13. ABE Dive 146 across the top of Cain Dome. ABE was deployed with a corner reflector both on the descent weight and also on a tether 3 meters tall. Once ABE was off and running we proceeded to Dredge target (K-40), Dredge DR-23.

After the dredge we maneuvered to monitor ABE. ABE appeared not to be moving, it looked stuck. ABE was remotely released from the bottom and was recovered and on deck by 12:33.
Proceeded to Dredge target (K-43), Dredge DR-24.
Repositioned the ship to launch ABE. ABE launched at 18:34. ABE Dive 147 was designed again to cross Cain Dome and to run along it for a magnetics run. While ABE was going down, JASON did a test lowering to 1000 m to test out the repaired tether (JASON Dive 115). The Jason engineers switched out one fiber for another fiber within the tether (there are 3 total). JASON checked out fine and ABE was checked and was doing fine.

JD339 - Sat 4 December 2004

Proceeded to Dredge target (K-30), Dredge DR-25. After the dredge we attempted to do a short sea surface maggie run. There were problems logging the data and this was compounded by over-writing of the data files collected, so we lost some data.
ABE signaled it was coming up at 12:31. ABE was on deck by 13:59. End of ABE Dive 147.
JASON was launched at 15:00. JASON Dive 116 from south to north across the surface of Cain Dome.

JD340 – Sun 5 December 2004

JASON Dive 116 continued.

JD341 - Mon 6 December 2004

End of JASON Dive 116. JASON on deck by 03:00.
ABE launched at 04:00. ABE Dive 148.
Proceeded to dredge target (K-44), Dredge DR-26.
Once dredge was on deck we went over and checked on ABE's progress. ABE's tracking looked good so we proceeded to do another dredge.
Proceeded to Dredge target (K45), Dredge DR-27.

JD342 - Tue 7 December 2004

ABE was coming up at 00:24. ABE was on deck by 20:21. End of ABE Dive 148.
Redeployed two transponders for Net#5. Surveyed the transponder net it.
Launched JASON for Dive 117 up a scarp south of Abel dome.

JD343 - Wed 8 November 2004

Waited for an elevator returning rocks from JASON. Recovered elevator at 13:14. JASON Dive 117 continued.

JD344 - Thu 9 December 2004

JASON was coming up at 03:31 and was on deck by 06:18. Recovered two transponders. End of JASON Dive 117.

Steamed over to ABE launch site. Launched ABE at 10:30. ABE Dive 149.
Proceeded to dredge target (K38), Dredge DR-28
Deployed the sea surface maggie for a short southern line across dive site and then drive back to listen to ABE.
ABE Dive 149 is finished.

JD345 – Fri 10 December 2004

Recover ABE at 02:04. Proceeded to recover the remaining three transponders. Done by 03:00. Begin transit back to Woods Hole.

JD346 - Sat 11 December 2004

In transit to Woods Hole. We took a track to SeaBeam survey across the New England seamount chain.

JD347 - Sun 12 December 2004

In transit to Woods Hole. NE seamount chain SeaBeam survey.

JD348 - Mon 13 December 2004

In transit to Woods Hole. NE seamount chain SeaBeam survey.

JD349 - Tue 14 December 2004

In transit to Woods Hole. NE seamount chain SeaBeam survey.

JD350 - Wed 15 December 2004

In transit to Woods Hole. NE seamount chain SeaBeam survey. At the end of the seamount chain we did a brief SeaBeam survey of shelf edge and Hydrographers Canyon.

JD351 - Thu 16 December 2004

In transit to Woods Hole. Continued the SeaBeam survey of shelf edge and Hydrographers Canyon.

JD352 - Fri 17 December 2004

07:00 Arrive in Woods Hole.

JASON DIVE PROGRAM SUMMARY

JASON DIVE 110

This dive was located on the north-south oriented, west-facing normal fault scarp that cuts across Babel megamullion dome at 23° 34.3’N, 45° 19.5’W. Prior to the Jason dive, ABE Dive 142 had completed a short mapping survey of the lower part of the scarp area using the SM2000 sonar. The Jason dive began at 2993 m depth and finished at 2905 m depth. Predominantly basalt talus was sampled at the base of the scarp. Basalt outcrop was encountered at ~2938 m. The dive was terminated due to mechanical problems. The oil compensation system had a leak and pressure had become too low to continue. At the surface it was found that a thruster had “knicked” one of the cables, allowing oil to escape. A total of 11 samples was taken. Total dive time was 5 hrs 58 mins.

JASON DIVE 111

This dive continued upslope from where Jason Dive 110 left off, and it continued to map and sample the west-facing normal fault scarp that cuts north-south across the Babel megamullion dome at 23° 34.3’N, 45°19.5’ W. The dive started at 2947 m depth and ended at the crest of the ridge at 2340 m depth. Like Jason Dive 110, mostly basalt talus was encountered on the lower reaches of the scarp. Outcrops of basalt became more prevalent upslope, especially in the areas indicated as steep by the ABE mapping at ~2850 m depth. The upper parts of the scarp showed in-place pillow lava tubes that flowed down hill (2780 m). A total of 20 samples was taken on the dive. Total dive time was 38 hrs 18 mins.

JASON DIVE 112

Dive 112 was located on the west-facing normal fault scarp that cuts through Cain megamullion dome at 23° 28.5’N, 45° 21’W. ABE Dive 144 had completed an extensive mapping program over this part of the scarp, which provided excellent morphologic context for the Jason Dive 112 sampling and mapping. The Jason dive began at a depth of 2918 m and reached the top of the scarp at 2275 m depth. The dive carried out several upslope traverses of the scarp wall, guided by the ABE mapping. A total of 116 samples was taken on the dive, and three elevators were used to return samples to the ship during the dive. Predominantly mantle rocks in the form of serpentinized peridotite were recovered from the scarp. The top of the scarp was covered with a carbonate deposit that restricted access to the underlying bedrock. Total dive time was 76 hrs 47 mins.

JASON DIVE 113

This dive traversed the steep east-facing side of Abel Dome, which is west of and directly adjacent to the previous dive and scarp on Cain Dome. We used the same transponder net for this dive. ABE Dive 145 had completed another detailed mapping survey of this portion of the slope before Jason Dive 113. The Jason Dive began at 2894 m depth and made one traverse up the slope and one across the face of the slope. A total of 73 samples was taken on this dive. One elevator was used to recover samples during the dive. Total dive time was 34 hrs 2 mins.

JASON DIVE 114
This dive was again on the east-facing slope of Abel Dome. The dive began at 2641 m depth at 23°N, 45°W. The dive first encountered some outcrop and then sloping fault surfaces. The dive was terminated due to electrical problems with the tether. The total sample count was 23 samples. Total dive time was 17 hrs 49 mins.

JASON DIVE 115
This dive was made down to 1000 m to test the repaired tether. Total dive time was 1 hr 46 mins.

JASON DIVE 116
This dive was located on Cain dome, crossing the megamullion fault surface from 23° 35'N, 45° 20'W. The dive began on mid-slope at 2415 m depth on the south-facing side of the dome. It climbed a basically south to north transect over the dome, and ended on the north-facing slope of the dome at 2273 m depth. A total of 52 samples were taken on this dive. Total dive time was 35 hrs 57 mins.

JASON DIVE 117
This dive was located on a very steep, west-facing scarp at 23° 23'N, 45° 25'W, southwest of the main megamullion domes. Two transects were made from the base of the scarp to the top of the scarp and then over the top onto the eastern slope which is interpreted to be a fault surface. On the first, southern, transect olivine gabbros and troctolites were sampled from 3390 m up to 2730 m, with diabase dikes appearing between ~3280 and 3090 m. Above 2710 m, diabases were recovered in 4 samples, with one basalt and one olivine gabbro at 2590 to 2950 m. On the second, northern, transect largely olivine gabbros and then troctolites were sampled from 3240 m upslope to 2820 m. Basalts occurred at 3130 to 3040 m. Upslope, one diabase was sampled at 2800 m, and only basalts were recovered above this depth. A total of 87 samples was taken on this dive, with one elevator used to recover samples in mid-dive. Total dive time was 48 hrs 19 mins.

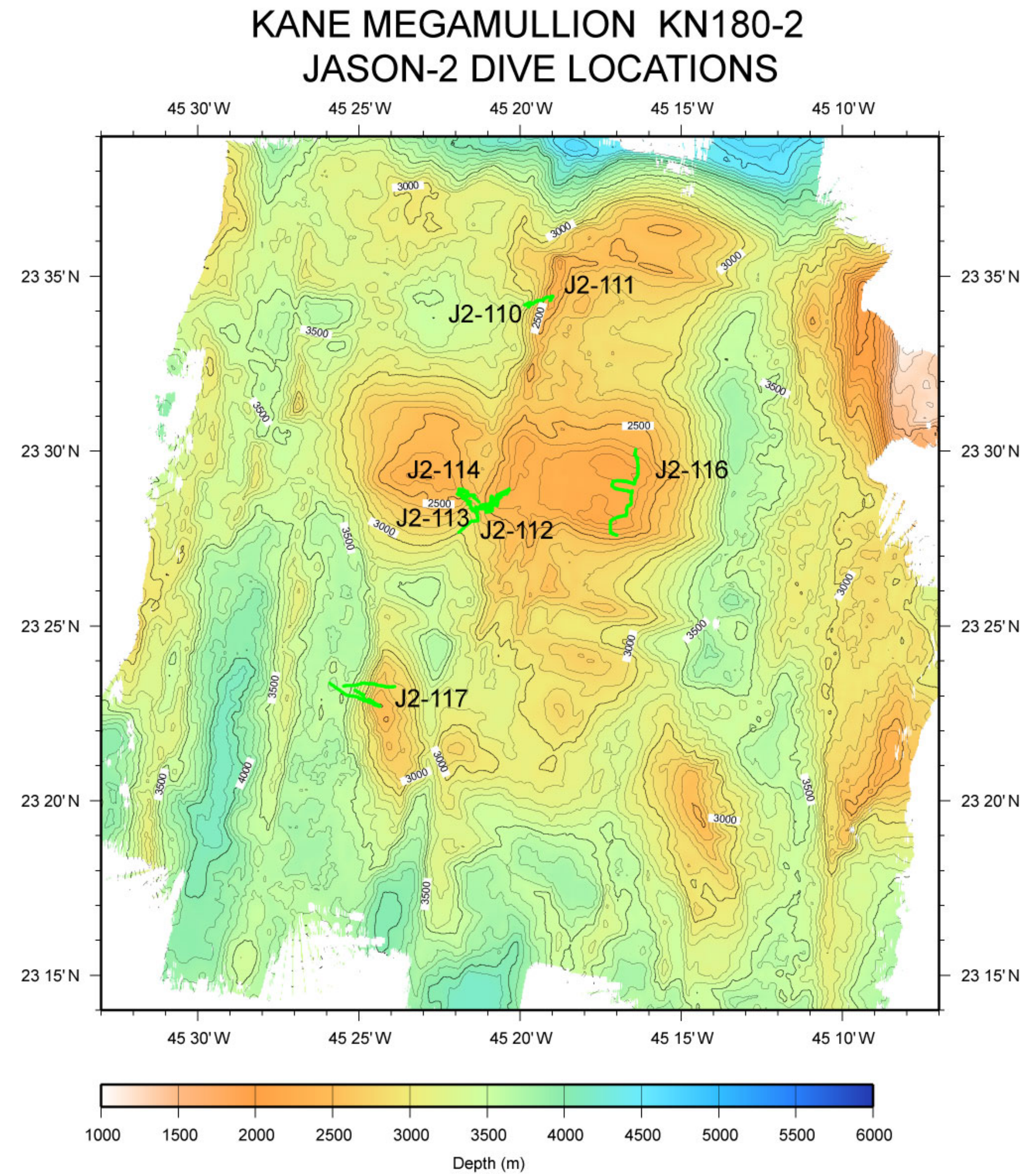

Figure 12. Seabeam map of study area showing the location of the Jason-2 dives.

ROCK SAMPLING SUMMARY

During the cruise 25 out of 28 dredges recovered some 1458.7 kg of rock, from which 756 individual samples representative of the full contents of each dredge were described in detail as included in the spreadsheets in the appendix. Seven Jason dives recovered 1207 kg of rock, and all 386 samples were described in detail as also included in the appendices to this report.

Thirty four percent of the igneous rocks collected were fresh (except for weathering) pillow basalts with little more than very-low grade brittle deformation. This contrasts sharply to the altered state of the plutonic and hyperbyssal rocks, and it is interpreted as signifying that many basalts are hanging-wall debris stranded on the Kane Megamullion detachment fault surface. The exception to this interpretation of basalts as debris are the basalts dredged and sampled from the long N-S trending fault scarp running from 23°25'N to 23°15'N and from 45°18.5'W to 45°24'W. Most of these could be interpreted as more recent off-axis eruptions on the basis of the identification of intact flow units on the wall of the scarp (Jason Dives 111 and 112), the physiography of the ridge, which is characteristic of constructional volcanic edifices, and the more frequent preservation of fresh basalt glass in pillow rims than in basalt debris from the detachment fault surface. In general, all basalts are typical mid-ocean ridge basalts, largely aphyric or sparsely phyric, with low vesicularity, typically less than 2 volume percent. Clinopyroxene was present only rarely as a phenocryst phase in the basalts, but small quantities of plagioclase and olivine were common.

Only 6% of the rock collected was diabase. For the most part these rocks were highly altered, typically in the greenschist facies, but extending to the lower amphibolite facies where crystal-plastically deformed. The scarcity of diabase at oceanic core complexes has been taken to suggest that sheeted dike complexes are rare at slow spreading ocean ridges. However the common association of diabase and gabbro and the preservation of numerous inliers of the dike-gabbro transition at Atlantis Bank suggests the alternative interpretation that detachment faults commonly root at the dike gabbro transition, and thus most diabase in the ocean crust was removed in the hanging wall and is preserved beneath the volcanic carapace found on the opposing tectonic plate. Our results are consistent with this observation, with diabase occurring in small quantities in many of the dredges across the detachment fault surface, and found intercalated with gabbros during Jason Dive 117 in a ~300 m exposure beneath the detachment fault surface where they comprised some 33.9% of the rocks collected. The dike-gabbro transition is typically around 500 m thick in ophiolite sections, consistent with this observation. While many diabases were aphyric, there were also abundant phyric and highly phyric varieties. This contrasts with the sparsely phyric to aphyric pillow basalts, but it is consistent with the observation made at Hess Deep that the dikes there have far more varied composition than spatially associated pillow basalts. This observation would seem entirely consistent with magma dynamics as density, viscosity, and magmatic overpressure should vary considerably with melt crystallization in the crust.

About 16% of the rocks collected are gabbroic. These include three principle varieties: 1) oxide gabbros and gabbronorites, 2) gabbro and olivine gabbro, and 3) troctolite and troctolitic gabbro. The gabbroic rocks sampled from the detachment fault surface have frequently experienced extensive retrogressive metamorphism, ranging from dry recrystallization in the upper amphibolite facies down to alteration to clay or complete replacement by soapstone in association with metaperidotites. From the large N-S fault scarps except in proximity to the detachment fault surface, however, they are often quite fresh with abundant olivine preserved, and they have undergone little recrystallization.

Olivine gabbro and gabbro (<5% modal olivine) are the most common variety of gabbroic rock sampled in the oceans, generally equivalent to the more differentiated MORB erupted along rift valleys. There they constitute about a third of the gabbros, representing roughly an appropriate proportion for in-situ crystallization of a parental mantle magma in the crust. The most common variety in our samples from the detachment fault surface, and as veins intruding peridotite was oxide gabbro with minor gabbronorite. These represent intrusion of highly evolved basaltic liquids that have previously undergone 70 to 80% fractional crystallization of parental MORB. Almost without exception, these rocks have undergone substantial crystal-plastic deformation, consistent with their intrusion along fault zones. Their consistent association with the detachment fault over large areas where mantle peridotite is the dominant rock type and where the most primitive gabbros are rare or absent argues that they are exotic to the section, and they could have been intruded from magma chambers located at depth and never exposed on the seafloor by faulting. However, the scarcity of dunites in the associated mantle rocks indicates that little vertical melt delivery occurred to the base of the crust in this region, and thus the likely source of the parental magmas for the oxide gabbros was an axial magma chamber located in the southern portion of this segment of the MAR.

Consistent with the latter interpretation was the collection of abundant gabbros by Jason Dive 117 and the dredges in this region. Some 48.3% of the rocks collected during the dive are gabbros, of which the large majority are primitive troctolites and troctolitic gabbros. These rocks are rarely found at oceanic transform walls, and are thus scarce in abyssal plutonic collections. At the 1.5 km deep Hole 735B, which was drilled entirely in gabbroic crust at the crest of the wall of the Atlantis Fracture zone in the Indian Ocean, almost none were found. This, and the scarcity of primitive gabbros in existing abyssal sample collections has given rise to the problem of the missing primitive cumulate. There is considerable speculation, fueled by the results of drilling gabbro plugs in mantle peridotite exposure during ODP Leg 209 near 15°N on the Mid-Atlantic Ridge, that the location of such cumulates is in the mantle. Here, however, we have found them as a crustal section exposed with sheeted dikes beneath the southern portion of the Kane Megamullion.

In contrast to a scarcity of dunites in the peridotites collected north of 23°25'N, dunites were found in abundance to the south, constituting 15.7% of dredges 21, 27 and 28. There were only three samples with dunite in the 14 dredges that recovered peridotite to the north. Dunite marks the locus of focused melt transport and delivery to the crust. Their close association with the abundant primitive gabbros sampled at Adam and Eve Knolls between 23°20' and 23°25'N, along with a large volcanic high on crust of the same age on the opposing tectonic plate provides convincing evidence for highly focused melt flow and delivery to the paleo-ridge segment.

Peridotite was the most abundant rock type sampled around the Kane Megamullion, constituting 42% of all rock collected. In general, the peridotites appear in hand-specimen to be highly depleted mantle harzburgites, with only a little lherzolite or plagioclase bearing peridotite found. This result, however, needs to be confirmed in thin section because the proportion of clinopyroxene in abyssal peridotites is notoriously difficult to determine by any other means. If clinopyroxene is indeed rare, it would be consistent with a significant transform edge effect inhibiting melting near fracture zones; the average Kane F.Z. peridotite was previously found to contain about 5.4% clinopyroxene (though this number is based on relatively few samples).

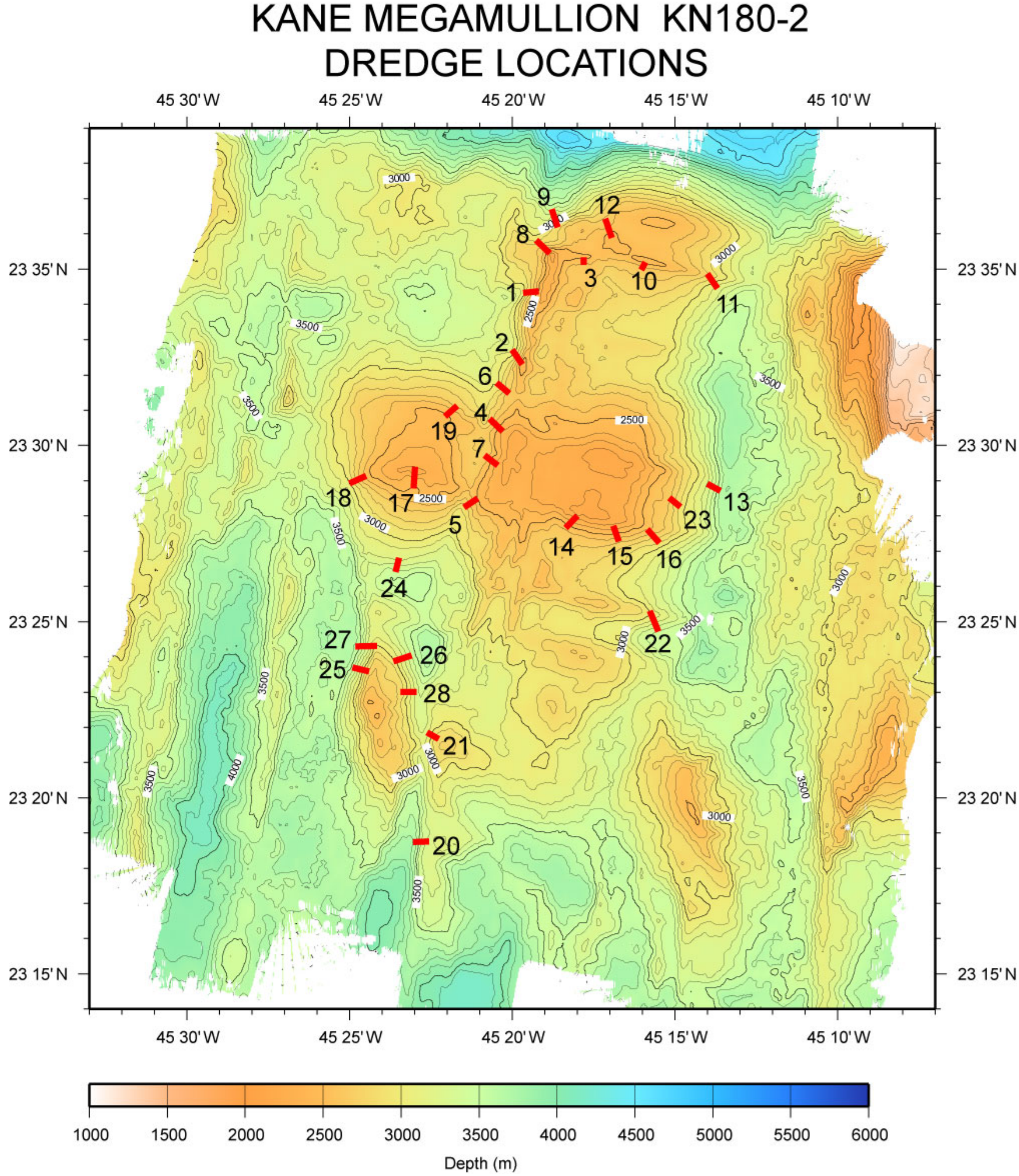

Figure 13. Seabeam map of the study area showing the location of rock dredges collected during the cruise.

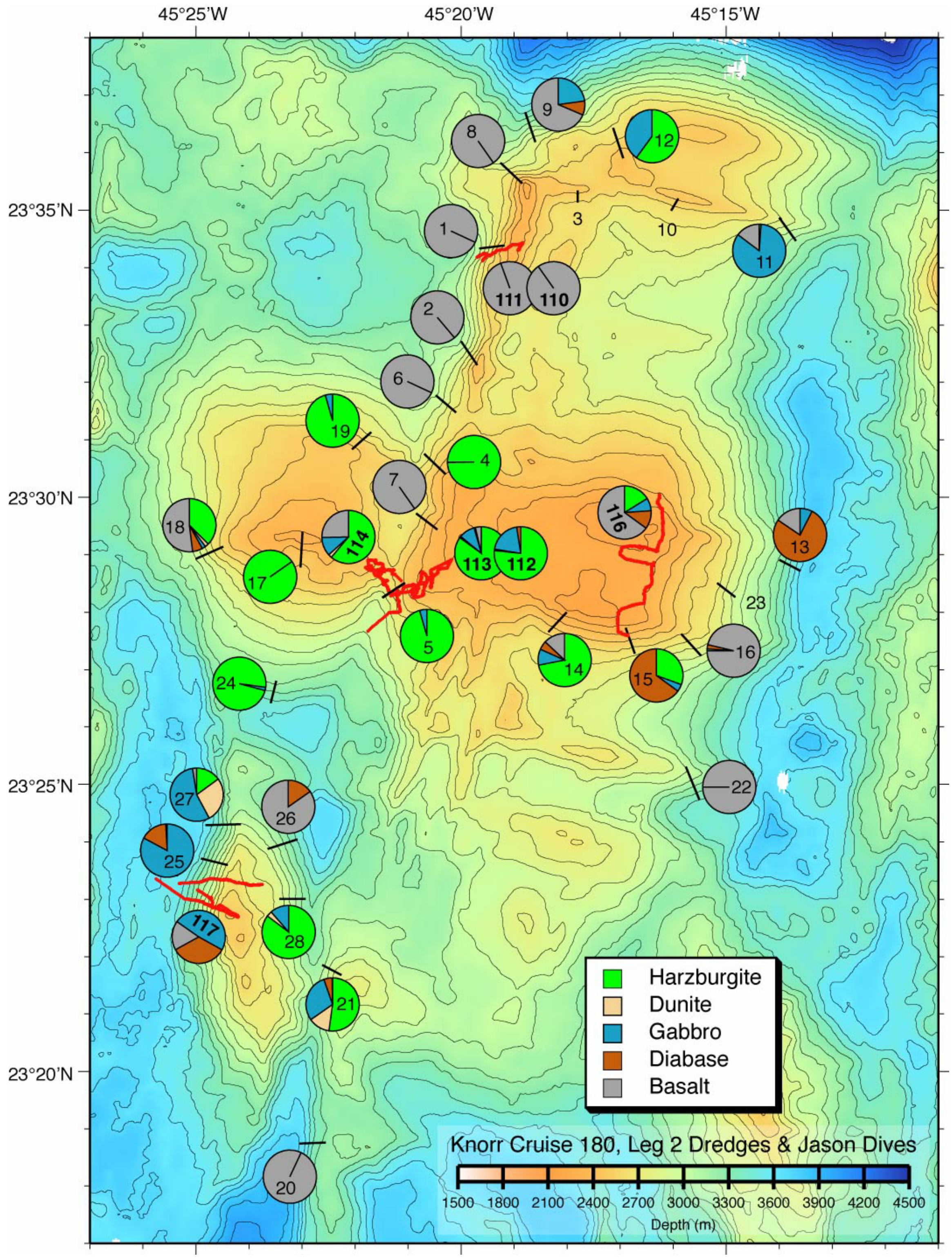

Figure 14. Seabeam bathymetry map with a summary of dredge and Jason rock sample lithology recovery.

ROCK SAMPLE DEFORMATION SUMMARY

The recorded rock deformation is discussed in four subsections:

i) the Cain and Abel Domes,
ii) the southern wall of the Kane Fracture Zone,
iii) south of 23^{o} 25'N
iv) Pillow basalts

Figure 15 provides a visual overview of the relative amounts of high temperature crystal plastic and lower temperature brittle deformation over the survey area.

i) The Cain and Abel Domes: Eleven dredges and four Jason dives provided an extensive data set for analysis of the deformation of the main detachment fault surfaces (Figure 15). Dives and dredges were either sited on the main detachment fault surface or on cross-cutting fault scarps. Jason dive 116 revealed that the uppermost surface of the Cain Dome is extensively sediment covered with only sparse undeformed pillow basalts exposed above the sediment cover. Dredges and dives on the postulated detachment surface on the eastern and southern margins of the dome recovered high temperature (>500^{o}C), amphibolite facies, peridotite and gabbro proto to ultra mylonites. High temperature strain appears to be preferentially localized in gabbro and oxide gabbro intrusions and veins when present. The high temperature deformation is extensively overprinted by low temperature (<400^{o}C) semi-brittle and brittle greenschist facies cataclasis. Samples and dive observations from Jason dive 113 suggest that this later deformation becomes localized into shear zones around more resistant boudins or facoids at both the hand specimen (10-30 cm) and outcrop (1-10 m) scale. Strain was localized onto the detachment fault by reaction-softening and fluid-assisted fracturing during greenschist- and subgreenschist-grade hydrothermal alteration of olivine, clinopyroxene, serpentine, and hornblende to tremolite, chlorite, and/or talc. Some, but not all, gabbros are only weakly deformed below amphibolite facies (<500^{o}C), indicating that strain is commonly partitioned into altered/metamorphosed peridotite at low temperatures.

Analysis of the deformation data suggest that rocks from the detachment fault surface are extensively overprinted by brittle deformation (dredges 13, 14, 15, 17, 18, 24 and Jason dive 116), whereas those from fault scarps cutting the detachment fault appear to show less brittle deformation (dredges 4, 5 and Jason dives 112, 113 and 114), suggesting that the semibrittle and brittle shear zones associated with the detachment fault are concentrated in the first 10-100 metres below the surface. This result is consistent with Schroeder and John's (2004) analysis of the Atlantis Massif detachment fault. However, we cannot constrain the thickness of the high temperature, crystal plastic zone of deformation. The rare occurrence of both deformed (dredge 13, Jason dive 116) and undeformed diabase within the detachment fault zone (Jason dive 116) suggests that detachment faulting was at least partly coeval with ridge magmatism.

ii) The southern wall of the Kane Fracture Zone: Dredges 9, 11 and 12 recovered non-volcanic crustal rocks from the northern flank of the Babel dome, on the southern wall of the Kane Fracture Zone. Dredge 9 recovered gabbros and diabases that had no deformation and are presumed to have come from beneath the detachment fault. Dredge 11 recovered an amphibolite facies proto-mylonitic gabbro with a static greenschist facies overprint. Dredge 12 recovered rocks with a weaker crystal plastic deformation and a stronger brittle deformation overprint than those from dredge 11. These rocks are presumed to be part of the detachment fault forming the upper surface of the Babel dome.

iii) Adam and Eve Knolls, south of 23^{o} 25'N: Adam's Knoll was the subject of a concentrated dredge and dive program. Dredges 26 and 28, on the eastern flank of the knoll, recovered diabases, which dominantly exhibit sub- and greenschist facies brittle deformation; undeformed, but highly weathered peridotites; and mylonitic gabbros with a greenschist facies brittle overprint. These dredges may have recovered rocks from the surface of a detachment fault, with the dominant brittle deformation indicating the close proximity of the fault to the breakaway. Dredges 25 and 27 and Jason dive 117 sampled a suspected west dipping fault scarp, which cuts the detachment fault. The recovered rocks are dominantly primitive gabbros and troctolites cross-cut by diabsae dikes. Deformation in these rocks is relatively rare; however high temperature gabbro mylonites were recovered from the dive and both dredges, and there is little evidence for a significant low temperature brittle overprint. Data from both slopes of Adam's Knoll are consistent with a model of relatively thin, detachment-related brittle deformation.

iv) Pillow Basalts: Pillow basalts are common over much of the region. They are found both on the detachment surface (Jason dive 116) and covering fault scarps which cut the Cain dome (dredges 1, 2, 6, 8, 20). The pillow basalts are essentially undeformed and unaltered. There are only two samples, which show deformation of the basalts by the detachment fault (Jason dive 116, Jason dive 117).

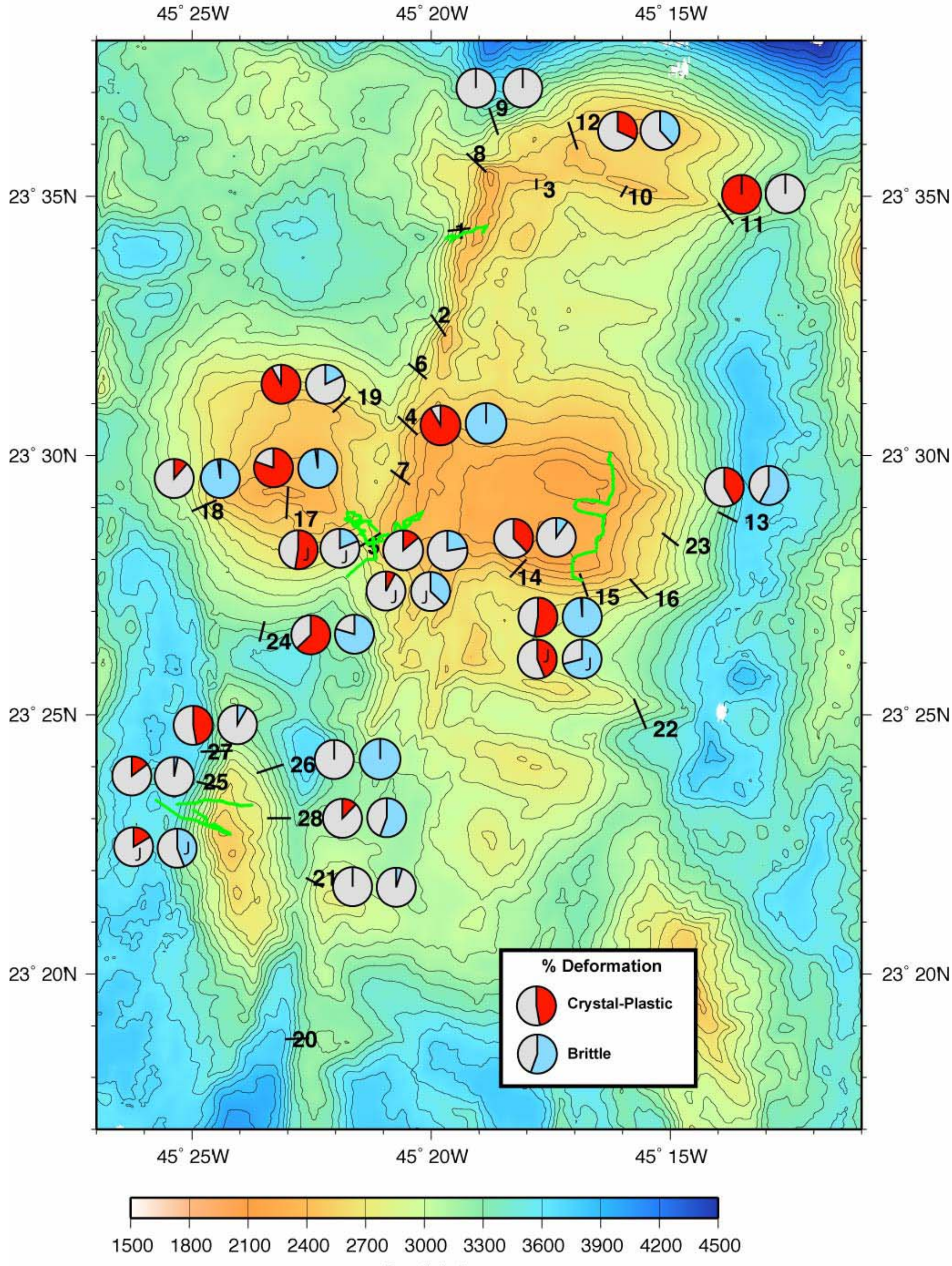

Figure 15. Map showing style of deformation, dredge locations and dive tracks in the survey area. Pie diagrams indicate the relative amount of crystal plastic (red) and brittle (blue) deformation in all non volcanic rocks. White areas indicate undeformed rocks. Red pie charts exclude perdidotites with a crystal plastic deformation grade of less than 2.

ABE DIVE PROGRAM SUMMARY

ABE made 8 dives at several sites in the Kane Megamullion study area. These dives covered a total of 175 km in 96 hours of bottom time. The primary sensors were 3-axis magnetometer, SM2000 multibeam sonar, a new chirp sub-bottom profiler, and a digital still camera. Operational details are included in Appendix-3 and Table 4. Below is a brief summary of the ABE dives.

ABE DIVE 142

ABE Dive 142 was located on the north-south oriented, west-facing normal fault scarp at 23° 34.3'N, 45° 19.5'W. ABE completed a short mapping survey of the lower part of the scarp area using the SM2000. Magnetic and sub-bottom data were also collected. Total survey time was 6.9 hrs.

ABE DIVE 143

This dive was designed to collect a near-bottom (10 m altitude) magnetic profile from east to west across the top of Babel megamullion dome. At the beginning of the dive, ABE completed a 5 m altitude camera-run south to north across the top of the dome in order to determine the sediment and type of rock outcrop present on the seafloor. Magnetic and sub-bottom data were collected but no SM2000 data. Total survey time was 13.2 hrs.

ABE DIVE 144

ABE Dive 144 was located on the west-facing normal fault scarp that cuts through Cain megamullion dome at 23° 28.5'N, 45° 21'W. ABE completed an extensive SM2000 multibeam mapping program over this scarp, providing an excellent morphologic context for the Jason Dive 112 sampling and mapping. Magnetic and sub-bottom data were also collected. Total survey time was 14.1 hrs.

ABE DIVE 145

This dive traversed the steep east-facing side of Abel Dome, which is west of and directly adjacent to the previous dive and scarp on Cain Dome. We used the same transponder net for this dive. ABE completed a detailed SM2000 survey of the slope. Magnetic and sub-bottom data were also collected on this dive. Total survey time was 14.9 hrs.

ABE DIVE 146

This dive was designed to cross the top of Cain dome from south to north and then to run a long east-west magnetic line. ABE only completed the cross line before encountering difficulties and having to be retrieved early. As part of the cross line, ABE deployed a small corner reflector and then surveyed with the SM2000 across the dome and the corner reflector before having problems. There were also sub-bottom problems also resulting in noisy data. Magnetic data were also collected. Total survey time was 2.38 hrs.

ABE DIVE 147

This dive was a low altitude (15 m) magnetic run from east to west across the top of the Cain dome. Sub-bottom data were also collected. No SM2000 data were collected. Total survey time was 13.66 hrs.

ABE DIVE 148

On this dive ABE completed three small "postage-stamp" sized surveys of potential drill targets on the top of Cain dome. The westernmost survey area was in a location thought to be dominated by basaltic volcanism, the second area was located at the magnetic transition where Jason Dive 116 and other ABE dives were located. The final area was located on the dome where it begins to slope down to the termination at the eastern end of the dome. At the end of these surveys ABE was supposed to run a high level magnetic line back west but unfortunately ran out of battery power before collecting the critical magnetic transition data. Sub-bottom data were collected throughout the survey. Total survey time was 16.24 hrs.

ABE DIVE 149

The last ABE dive of this cruise was to complete a high level magnetic run across the top of the Cain dome. ABE first filled in a few SM2000 survey lines at the central postage-stamp survey area where Jason Dive 116 had also visited. ABE then ran the high level line. No sub-bottom data were collected due to equipment failure. Total survey time was 11.34 hrs.

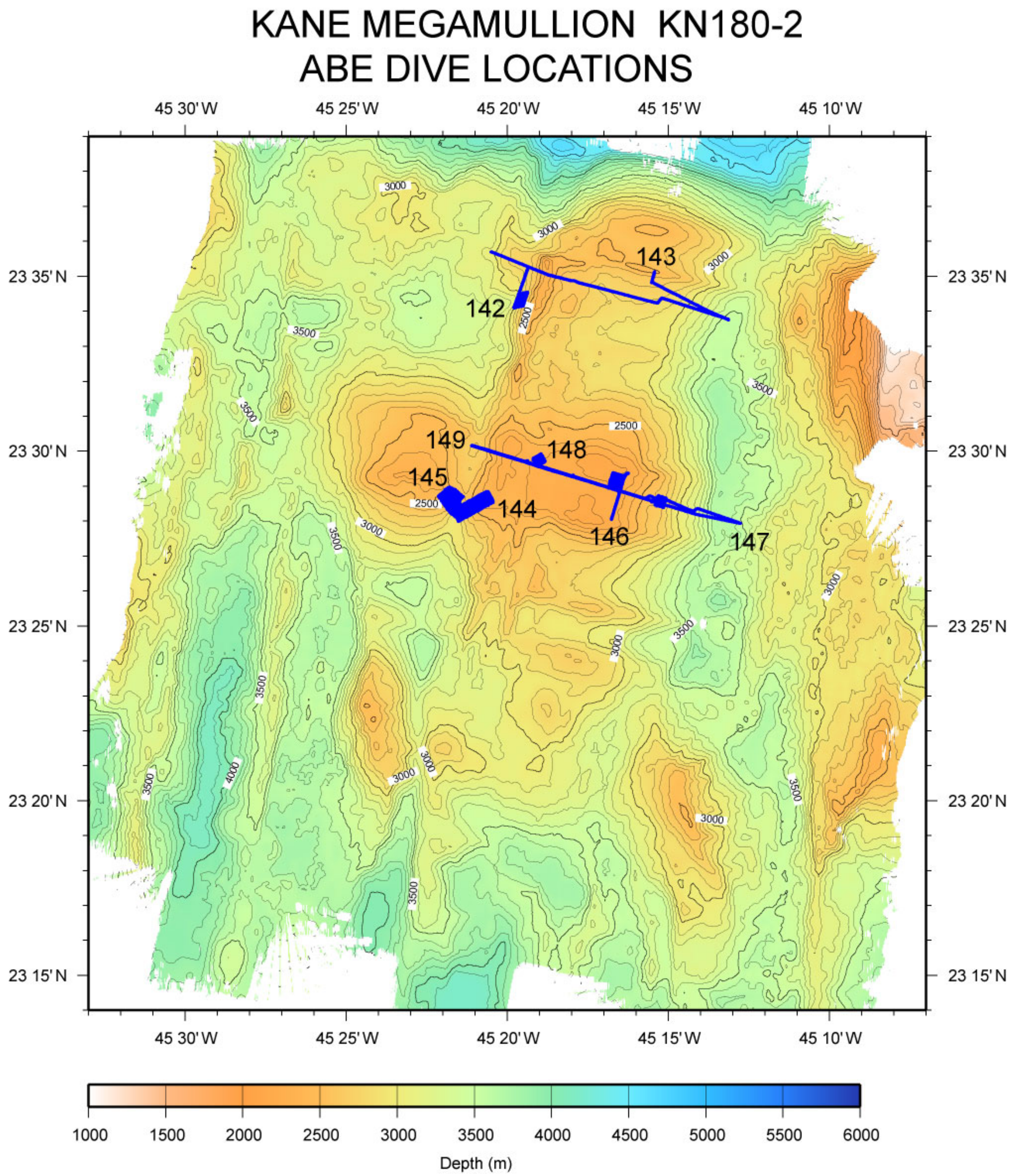

Figure 16. Seabeam map of the study area showing the location of the ABE dives.

MAGNETIC FIELD MAPPING SUMMARY

Multiple magnetic datasets were acquired during this cruise using a sea-surface magnetometer and magnetometers mounted on both ABE and Jason. Sea surface magnetic data were recorded throughout the survey area. ABE collected both near-bottom magnetic data grids and single track lines across the megamullion structure, parallel to flow-line at varying heights above seafloor. Jason recorded near-bottom magnetic data along all its dive tracks (see Figures 12 and 16)

Average magnetic values at the survey area 23° 30'N 45° 20'W:

Geomagnetic Field: 37650 nT
Inclination: 40.77°
Declination: -16.67° (i.e. west of north)

Sea Surface Magnetic Data

The sea surface magnetic data were recorded by an Overhauser magnetometer, which records absolute geomagnetic field values (Figure 9). The magnetometer was streamed 1000 ft behind the ship and towed at a speed of 10 knots in the study area. Data were logged onboard the R/V Knorr in real time with a sampling frequency of 1 Hz. GPS data were also logged with the same sampling frequency to provide position data.

The first sea surface magnetic data were collected during the initial SeaBeam survey of the study site (Julian Day 322 to 324). Figure 17 shows two profiles from this survey, Lines 1 & 3. On Day 334 a third profile located between and parallel to the earlier lines was acquired (Line 2). A final line, Line 4, was collected on Day 344 at the southern end of the survey area.

Sea surface magnetic data from a previous cruise, Ewing 01-02, are also included in Figure 17. These combined data illustrate a consistent pattern in the anomalies throughout the study area, perpendicular to the spreading axis and parallel to the transform fault. All profiles show a change in polarity of the anomalies around the location of the megamullion. We note here that the observed magnetic data need to be phase shifted (i.e. reduced-to-the-pole) to center the anomalies over the causative body.

ABE and Jason Magnetic Data

A Develco fluxgate (3-axis) magnetometer was mounted at the front of the main ABE body. The orientation of the magnetometer was:

```
x-channel =  ABE positive starboard (Y-axis east)
y-channel =  ABE positive forward (X-axis north)
z-channel =  ABE vertical up (-Z-axis vertical).
```

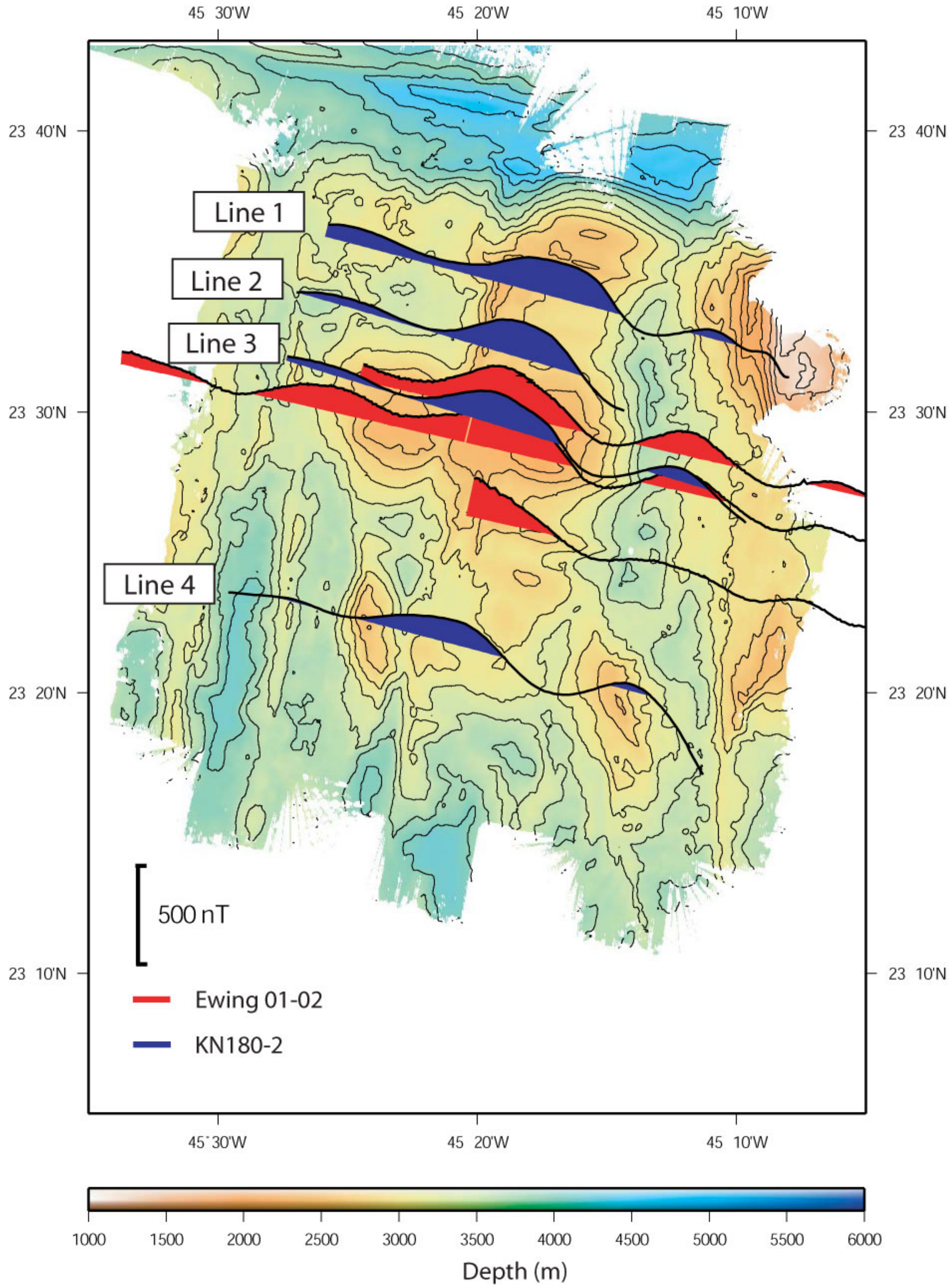

Figure 17. Sea surface magnetic anomalies measured across the study region. Filled wiggles are positive anomalies with red color indicating the Ewing 01-02 cruise data and blue color data collected on this cruise KN180-2.

The ABE magnetic data were recorded at a sampling frequency of 1 Hz.

On Jason an HMR 2300 Honeywell magneto-resistor (3-axis) magnetometer was mounted at the top, front, port side of the vehicle (see Figure 4). The orientation of the magnetometer was:

```
x-channel = -Z axis vertical
y-channel = -Y axis east
z-channel = -X axis north
```

The Jason magnetic data were recorded at a sampling frequency of 1 Hz.

Site 1- Basalt Ridge - ABE 142, J2-110, J2-111

ABE conducted a grid survey of Site 1, approximately 50 m above the seafloor. The permanent and induced effects of the vehicle were removed by fitting a cosine curve to the ABE heading data. The magnetic effect of the vehicle was reduced from ~800 nT to ~20 nT. These data were upward continued to 2.7 km water depth and reduced to the pole (Figure 18). The anomaly has a positive gradient from SW to NE (upslope direction). Jason dives J2-110 and J2-111 were in the same area. The magnetic data from Jason Dive 111 has the same positive slope as the ABE grid, in the upslope direction (Figure 19). A sharp peak at ~2750 m water depth may represent a polarity boundary or contact of some kind.

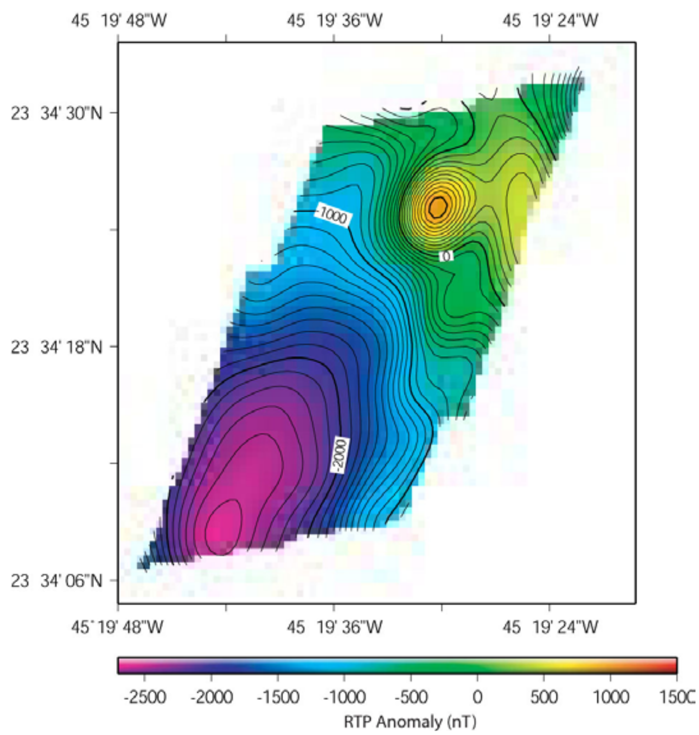

Figure 18. ABE Dive 142 upward continued and reduced to the pole anomaly map.

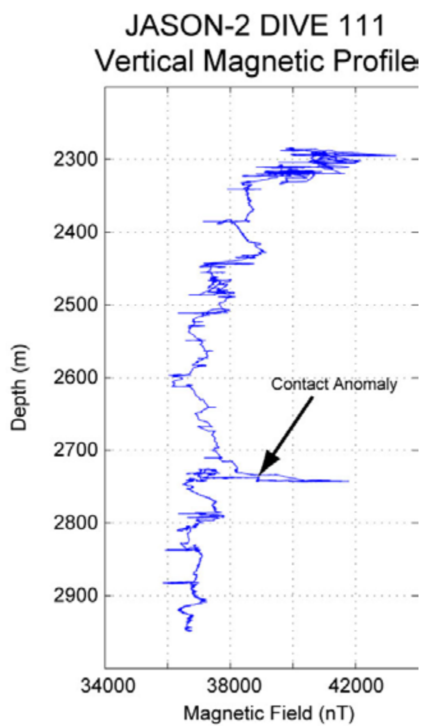

Figure 19. Vertical magnetic profile from Jason Dive 111 showing a distinct magnetic boundary at approximately 2750 meters depth, possibly a magnetic reversal or a lithologic contact.

Track 1- Babel dome - ABE 143

One of the main scientific objectives of the cruise was to collect multiple magnetic profiles at various water depths across the megamullion in order to determine dip of the subsurface detachment fault. 'Line 1' was first recorded by a sea-surface magnetometer as mentioned above. Near-bottom data along the same line were recorded during ABE 143 (20 m above the seafloor). Figure 20 shows both the sea-surface and near-bottom profiles. Both have the same

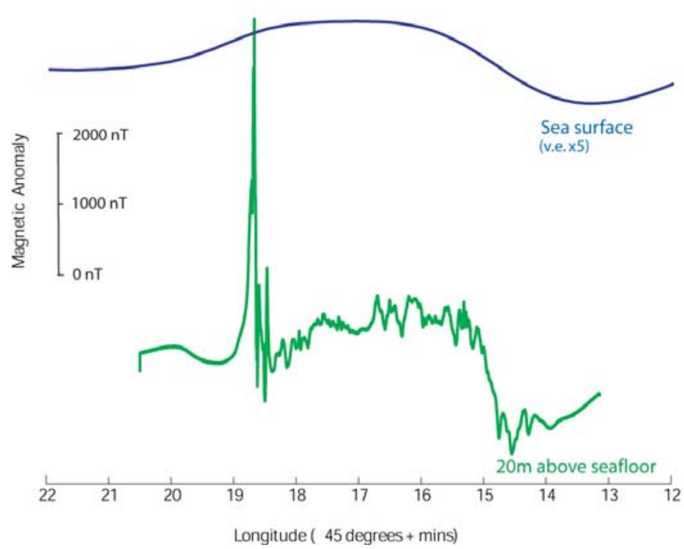

Figure 20. ABE magnetic profile compared to sea surface profile over northern Babel Dome.

long wavelength appearance with a polarity change around 45° 15’W. The near-bottom profile has an interesting peak, which coincides with the location of the basalt ridge in the north of the survey area.

Site 2- Cain and Abel flanks – ABE 144, ABE 145

ABE completed two grid surveys of the flanks on each of the domes. These grids are combined in Figure 21. The data were continued to 2.2 km water depth and reduced to the pole. The data show positive gradients in the upslope direction, the same as the grid at Site 1. This suggests that the anomalies are due to topographic features and this contribution can be removed during an inversion.

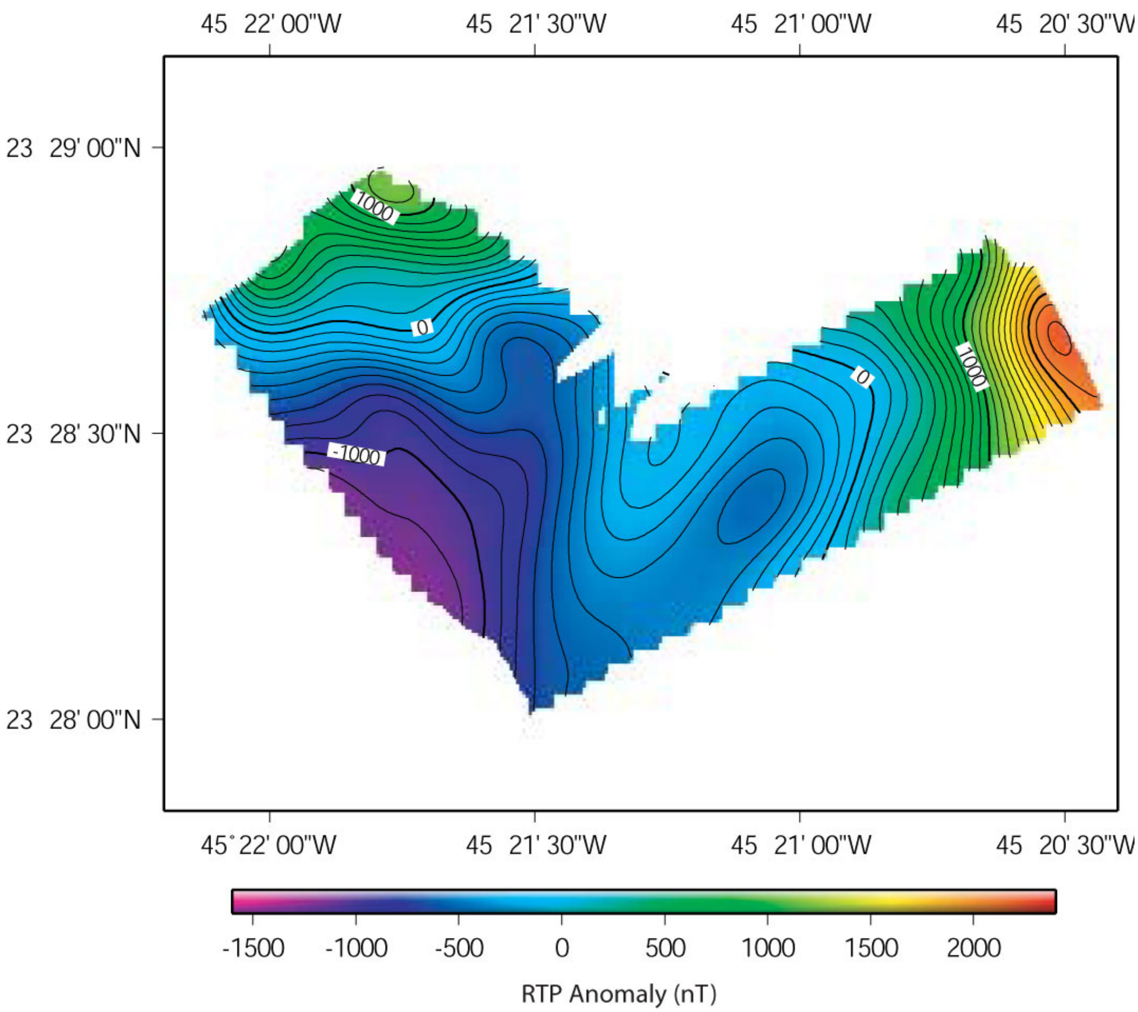

Figure 21. ABE dive 144 magnetic field data combined with ABE dive 145 data. The magnetic data have been upward continued and reduced to the pole.

Track 2- Cain dome - ABE 147, ABE 148, ABE 149

During three dives ABE acquired magnetic profiles along 'Line 3' at 20 m above seafloor (ABE147), 60 m above seafloor (ABE148), and 250 m above sea-floor (ABE149). These data, and the sea-surface data along the same line, are shown in Figure 22. This figure illustrates the gradual broadening and smoothing of the anomalies with increasing distance above the seafloor. The polarity boundary at approximately 45°17'N is the dominant long-wavelength feature in all the profiles. ABE 148 also surveyed three small grids at the proposed drill site locations (Figure 23.).

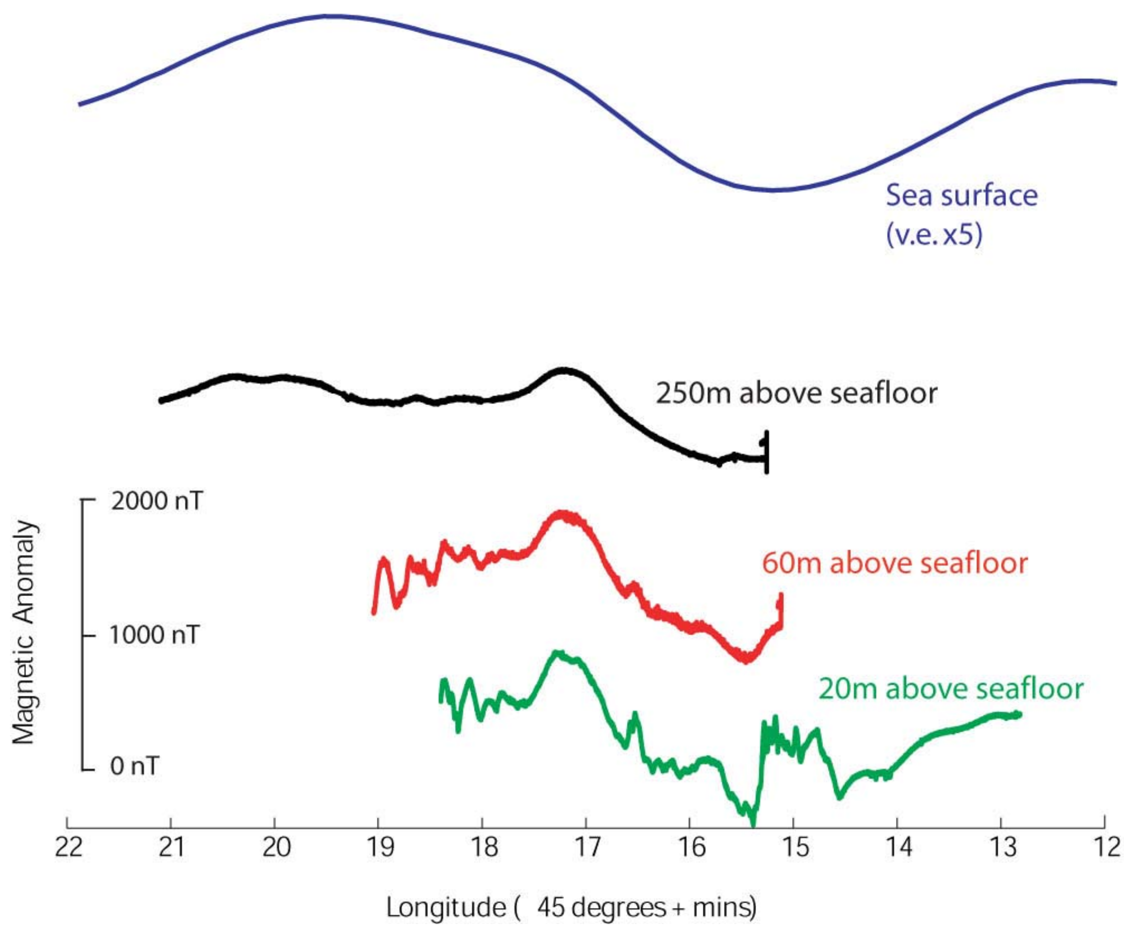

Figure 22. Near bottom magnetic profiles collected as various levels across the top of the main Cain megamullion dome showing the location of the young edge of chron 2A reversal boundary.

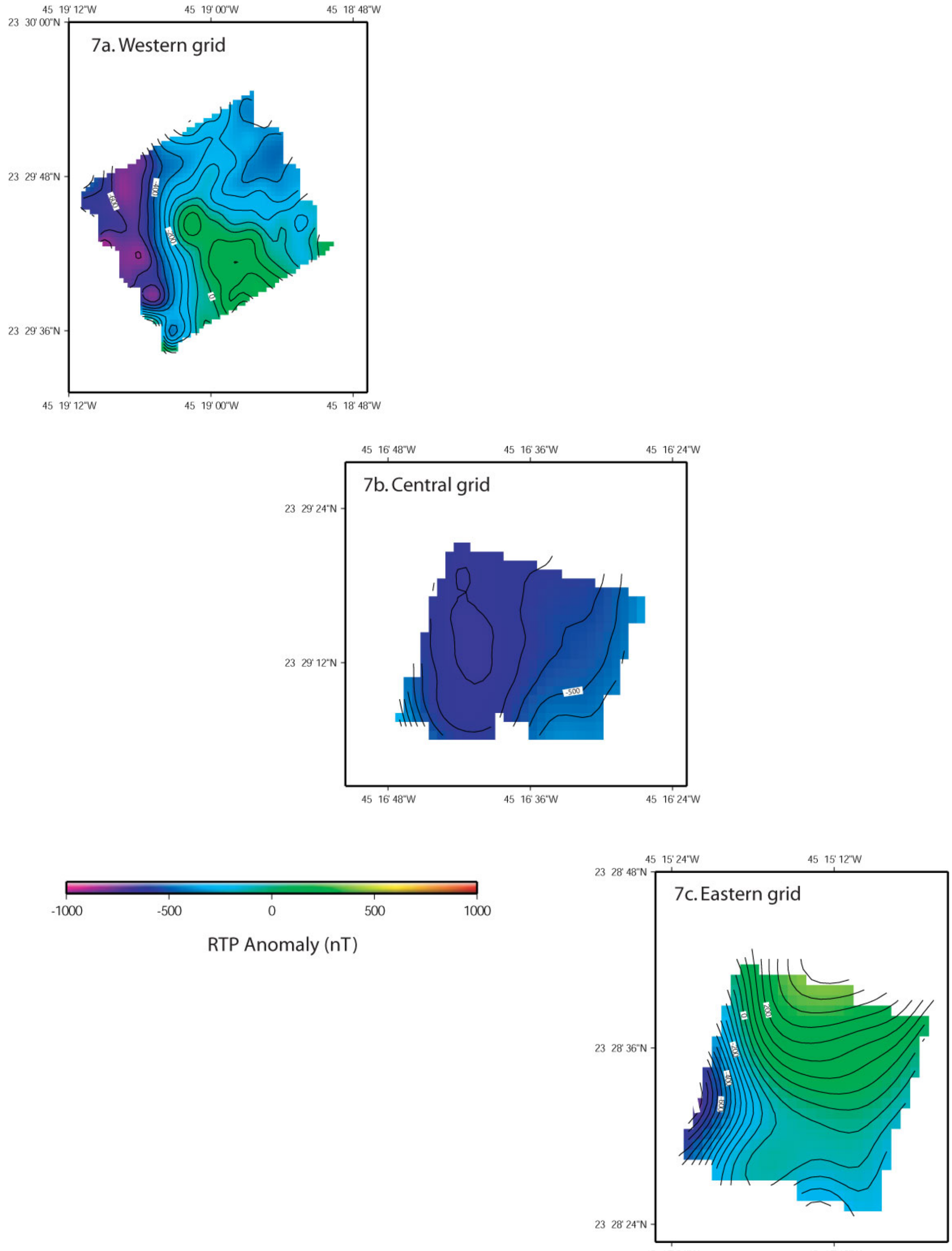

Figure 23. ABE Dive 148 magnetic field data over three detailed proposed drilling sites. Data has been upward continued and reduced to the pole.

CRUISE REPORT RECOMMENDATIONS

Jason Operations

First and foremost, the Jason team must be congratulated for an excellent effort in collecting samples and navigating up steep slopes that were difficult in some circumstances. The entire team was responsive to our needs where practical in both operations and the set-up of lights, cameras, etc. We were able to take samples in the majority of circumstances. The pilots did a good job of keeping track of the payload and letting science know what the impact of sampling would have for the ensuing hour of operation. There were no weather issues on the cruise. There were a few vehicle problems most notably with the oil compensation system, which forced recovery in two circumstances but we never felt that the vehicle was limited in power for collecting samples or for mapping. In summary, the new Jason-2 is a remarkable improvement over its earlier namesake. The DVD recording system worked very well as did the duping system and the labeling system. These are a great improvement over previous tape-based archiving systems.

We do, however, have a number of recommendations that we feel could make the vehicle more useful for science and generally these are incremental changes that would not require significant resources. For operations such as ours where we were doing geological and structural mapping, accompanied by rock sampling, there are several specific improvements in Jason operations that would tremendously enhance the scientific return. These include the following.

The Medea video image often provided a scientifically useful overview of the terrain surrounding Jason and this could be used in a mapping sense to extend the mapping done with Jason. Unfortunately, the Medea image was usually overexposed by the lights of Jason and was not recorded in real time like the other video sources (although a framegrab was taken every 30 seconds). Our recommendations include:

- Replacing the Medea low light camera with a video camera that can cope with the dynamic range in lighting from Jason-2. Currently the forward lighting from Jason saturates the image so all seafloor features in that direction are washed out. We note that there have been studies done on using a light before the camera (LIBEC) configuration and perhaps this could be looked into.

- The output from the Medea camera should be recorded routinely and continuously as part of the video data stream. This recording should be in addition to, and not at the expense of, the current video recording capabilities.

- Additional lighting should be added to the sides of Jason-2 so that the entire seafloor around the vehicle is illuminated and thus visible to the Medea video camera. This would make it possible readily to correlate visual imagery of the seafloor with fine-scale seafloor bathymetric features mapped by the ABE SM2000.

On the other video cameras we found that:

- The Science pan/tilt video camera did not have effective automatic iris control or the resolution of the Pilot pan/tilt video. This could be due to the difference in monitors or lighting. The Science pan/tilt camera should provide video quality equal to or better than the Pilot pan/tilt video camera.

- Both the Science and Pilot pan/tilt video cameras should provide information on image orientation (azimuth and dip with respect to the horizontal).

- The zoom control on the control box for the Science pan/tilt video camera should be oriented so that pushing the rocker button *forward* causes the camera to *zoom in*, and pushing it *to the rear* causes to camera to *zoom out*. This is currently backward, is counterintuitive, and caused considerable confusion.

- A digital still camera (DSC) with much greater image capacity should be used on Jason. The DSC used on our cruise was loaned to the DSL group by Dan Fornari and had a capacity of only 1200 frames and needed to be downloaded after each dive. This required us to conserve frame space by turning the camera off each time the vehicle stopped to sample and then turning it back on when Jason began to move again. This was an unnecessary, additional chore in the Jason van, and failure to remember it sometimes caused loss of data.

- It would be helpful to have the SM2000 shut off automatically when Jason stops moving (e.g, for sampling outcrop) and then start again when Jason begins moving. Turning the SM2000 off and on at each sample location, like doing so with the DSC, is an unnecessary chore and can result in data loss.

- The sample elevator worked well, but it could be improved by making the plywood boxes a few inches larger and by inserting 'teflon' or UHMW ramps at high angles around the insides of the boxes to make inserting and removing baskets easier. This would be particularly helpful when the elevator is canted on a seafloor slope.

- One claw on each of Jason's manipulators should be painted. This will help in orienting samples removed from outcrops, particularly when sampling is obscured by mud clouds, overhangs, or poor video quality.

- Inside the van, a better lighting setup is needed over the map table. Gooseneck lights should be permanently mounted above the table. Also the vehicle position/status (DVLNAV) display used by the science watch should be mounted at the forward end of the 'science table' in an orientation readily visible from the position where the watch leader sits by the map table.

- For our cruise report, and for those cruises that use Jason in the future, the Jason team should provide an operations summary that includes any problems encountered and repairs made.

- The Virtual Van web-based summary was a very useful tool for scrolling through the data and video information collected during the ROV dives. However, it became increasingly unwieldy to have to scan through the entire series of dives. It would have been much easier to have kept each dive as a separate entity. It would also be useful to archive the virtual van records for each Jason dive onto a CD or DVD so that we could use it off-line and to have a backup disk for each dive similar to the ALVIN configuration. Another issue arose at the end of the cruise when the Jason team wanted to pack up the system and shut down the computers providing the virtual van data. This was unsatisfactory to science. We negotiated a two-day phase out period, but in reality there should be no such reason to have this removal of the service before the end of the cruise. In our case, Tom Bolmer did us a tremendous service by getting the Virtual Van running on a computer outside of the Jason van, which allowed us to finish the cataloging of samples and analysis that we needed to perform before the end of the cruise.
Navigation data was an issue. The first Jason dive 110 had no useful Jason navigation but did have Medea navigation. The second dive had better Jason LBL navigation and some doppler velocity log (DVL) navigation, but the doppler we were using did not have the range for the terrain we were studying, i.e. steep scarps. The Jason team added a lower frequency 300 khz Doppler that we used for the rest of the program which improved the DVL navigation considerably. We would recommend having this option for future dive programs especially in steep terrain.

A second issue was how the navigation data was presented to us and when. It was unclear who was responsible for getting processed navigation and a dive track to the science party. There are several different types of navigation data structures from LBL to DVL for Jason to LBL for Medea and GPS for the ship. Combining and making sense of all these different data sets is a complex and daunting task. The Jason group is in the best position to know which of these is the more reliable and when. For those science groups not used to dealing with MATLAB and data intensive operations, processing the navigation and obtaining a simple track of the vehicle would be a daunting task. It would be our recommendation that the Jason team provide a track map of the raw navigation and then edited navigation track. These track maps could be devoid of bathymetric features (contours) if need be or could include the terrain if provided by the science group beforehand. The navigation watch for Jason could process the data and then provide the Jason data person with the appropriate navigation data to plot out on track map for science.

Clear documentation on all the data record records needs to be provided. There were some data strings and file formats that were not listed in the typical Jason spreadsheet. More information is needed.

ABE operations

- The newly installed chirp subbottom profiler provided useful data on sediment thickness, which seems to have been a few meters at most. Most data were clean, but one data set recorded during Dive 146 was very noisy. The source of this noise should be determined and eliminated.

- ABE provide high-quality photography. Many frames, however, showed tares in the centers or bottoms of images. The cause of these errors should be determined and eliminated.

- The crane used to launch and recover ABE on the starboard waist deck leaves a lot to be desired. The crane operates with the boom up at a very high angle and with a very long cable so that ABE swings strongly even with tag lines attached. This is not a good system. It presents a danger to both personnel and to the vehicle itself.

REFERENCES

Allerton, S. and M. A. Tivey, Magnetic polarity structure of lower oceanic crust, *Geophys. Res. Lett., 28*, 423-426, 2001.

Auzende, J.-M., et al., Observation of sections of oceanic crust and mantle cropping out on the southern wall of Kane FZ (N. Atlantic), *Terra Nova, 6*, 143-148, 1994.

Cann, J. R., et al., Corrugated slip surfaces formed at ridge-transform intersections on the Mid-Atlantic Ridge, *Nature, 385*, 329-332, 1997.

Casey, J. F., et al., Megamullions along the Mid-Atlantic Ridge between 14 and 16N: Results of Leg 1, JAMSTEC/WHOI Mode 98 survey (abstract), *EOS Trans. AGU, 79, No. 45 (Fall Meeting Supplement)*, F920, 1998.

Dick, H. J. B., et al., Evidence for a "melt lens" equivalent in the lower crust at an ultraslow spreading ridge (abstract), *EOS Trans. AGU, 80, No. 46 (Fall Meeting Supplement)*, F956, 1999.

Fujimoto, H., et al., Gravity anomalies of the Mid-Atlantic Ridge north of the Kane Fracture Zone, *Geophys. Res. Lett., 23*, 3431-3434, 1996.

Fujimoto, H., et al., Preliminary results from the first submersible dives on the Southwest Indian Ridge (abstract), *EOS Trans. AGU, 79, No. 45 (Fall Meeting Supplement)*, F893, 1998.

Gao, D., et al., Computer-aided interpretation of side-looking sonar images from the eastern intersection of the Mid-Atlantic Ridge with the Kane transform, *J. Geophys. Res., 103*, 20,997-21,014, 1998.

Gente, P., et al., Characteristics and evolution of the segmentation of the Mid-Atlantic Ridge between 20°N and 24°N during the last 10 million years, *Earth Planet. Sci. Lett., 129*, 55-71, 1995.

Harrison, C. G. A., Marine magnetic anomalies - the origin of the stripes, *Ann. Rev. Earth Planet. Sci., 15*, 505-543, 1987.

Karson, J. A., et al., Deep-Tow operations at the eastern intersection of the Mid-Atlantic Ridge and the Kane Fracture Zone (abstract), *EOS Trans. AGU, 73*, 552, 1992.

Karson, J. A., Geological investigation of a lineated massif at the Kane transform fault: Implications for oceanic core complexes, *Philos. Trans. R. Soc. London, 357*, 713-740, 1999.

Kent, D. V., B. M. Honnorez, N. D. Opdyke and P. J. Fox, Magnetic properties of dredged oceanic gabbros and the source of marine magnetic anomalies, *Geophys. J. R. Astron. Soc., 55*, 513-537, 1978.

Kikawa, E. and K. Ozawa, Contribution of oceanic gabbros to sea-floor spreading magnetic anomalies, *Science, 258*, 796-799, 1992.

Maia, M. and P. Gente, Three-dimensional gravity and bathymetry analysis of the Mid-Atlantic Ridge between 20°N and 24°N: Flow geometry and temporal evolution of the segmentation, *J. Geophys. Res., 103*, 951-974, 1998.

Manning, A. H. and J. M. Bartley, Postmylonitic deformation in the Raft River metamorphic core complex, northwestern Utah: Evidence of a rolling hinge, *Tectonics, 13*, 596-612, 1994.

Mitchell, N. C., J. Escartín and S. Allerton, Detachment faults at mid-ocean ridges garner interest, *EOS Trans. AGU, 79*, 127, 1998.

Morris, E., R. S. Detrick and B.-Y. Kuo, Three-dimensional analysis of gravity anomalies in the MARK area (Mid-Atlantic Ridge, 23°N), *EOS Trans. AGU 70*, 1326, 1989.

Pariso, J. E. and H. P. Johnson, Do layer 3 rocks make a significant contribution to marine magnetic anomalies? In situ magnetization of gabbros at Ocean Drilling Program Hole 735B, *J. Geophys. Res., 98*, 16,033-16,052, 1993a.

Pariso, J. E. and H. P. Johnson, Do lower crustal rocks record reversals of the Earth's magnetic field? Magnetic petrology of oceanic gabbros from Ocean Drilling Program Hole 735B, *J. Geophys. Res., 98*, 16,013-16,032, 1993b.

Pockalny, R. A., R. S. Detrick and P. J. Fox, Morphology and tectonics of the Kane transform from SeaBeam bathymetry data, *J. Geophys. Res., 93*, 3179-3193, 1988.

Pockalny, R. A., A. Smith and P. Gente, Spatial and temporal variability of crustal magnetization of a slowly spreading ridge: Mid-Atlantic Ridge (20°-24°N), *Mar. Geophys. Res., 17*, 301-320, 1995.

Schroeder, T., B. and John, B.E., 2004, Strain localization on an oceanic detachment fault system, Atlantis Massif, 30°N, Mid-Atlantic Ridge; G3, 5, 11, doi:10.1029/2004GC000728.

Schulz, N. J., R. S. Detrick and S. P. Miller, Two- and three-dimensional inversions of magnetic anomalies in the MARK area (Mid-Atlantic Ridge 23°N), *Mar. Geophys. Res., 10*, 41-57, 1988.

Searle, R. C., et al., TOBI sidescan imagery and magnetics of the Southwest Indian Ridge III: Detailed history and tectonic style of seafloor spreading and detachment faulting, 0-3 Ma, 63°30'-63°56'E (FUJI Box 3) (abstract), *EOS Trans. AGU, 79, No. 45 (Fall Meeting Supplement)*, F855, 1998.

Sempéré, J.-C., D. Christie and B. P. West, Unpublished geological and geophysical survey data of Australia-Antarctic Discordance, Southeast Indian Ridge, 1998.

Talwani, M., C. C. Windisch and M. G. Langseth, Reykjanes Ridge crest: A detailed geophysical study, *J. Geophys. Res., 76*, 473-517, 1971.

Tivey, M. A. and B. E. Tucholke, Magnetization of 0 to 29 Ma ocean crust on the Mid-Atlantic Ridge at 25°30' to 27°10'N, *J. Geophys. Res., 103*, 17,807-17,826, 1998.

Tucholke, B. E., et al., Segmentation and crustal structure of the western Mid-Atlantic Ridge flank, 25°25'-27°10'N and 0-29 m.y., *J. Geophys. Res., 102*, 10,203-10,223, 1997a.

Tucholke, B. E., W. K. Stewart and M. C. Kleinrock, Long-term denudation of ocean crust in the central North Atlantic Ocean, *Geology, 25*, 171-174, 1997b.

Tucholke, B. E., K. Fujioka and T. Ishihara, Shinkai 6500 dives on Dante's Domes, a megamullion in the eastern rift mountains of the Mid-Atlantic Ridge at 26.6 degrees North (abstract), *EOS Trans. AGU, 79, No. 45 (Fall Meeting Supplement)*, F45, 1998a.

Tucholke, B. E., J. Lin and M. C. Kleinrock, Megamullions and mullion structure defining oceanic metamorphic complexes on the Mid-Atlantic Ridge, *J. Geophys. Res., 103*, 9857-9866, 1998b.

Table 2. Transponder coordinates for Jason and ABE operations KN180-2.

For all acoustic transponder nets the XY Origin was defined as:
23º 28.00' N 45º 22.00' W UTM Zone 23

Table 2a. Transponder Net #1
This net configuration was used for Jason Dives 110,111 and ABE Dive 142

ID	Latitude	Longitude	Depth (m)	X (m)	Y (m)
A (11.5)	23º 33.73526' N	45º 20.32477 'W	2947.4	2852.6	10585.9
B (9.5)	23º 35.28714' N	45º 20.13708 'W	2692.9	3172.2	13450.3
C (10.0)	23º 33.39571' N	45º 18.83094 'W	2080.7	5396.3	13650.7
D (8.5)	23º 33.87262' N	45º 16.65505 'W	2517.3	9101.4	12685.2

Table 2b. Transponder Net #2
This net configuration was used for ABE Dive 143

ID	Latitude	Longitude	Depth (m)	X (m)	Y (m)
A (11.5)	23º 32.8610' N	45º 15.9620 'W	2621.7	2852.6	8972.2
B (9.5)	23º 35.28714' N	45º 20.13708 'W	2692.9	3172.2	13450.3
E (10.0)	23º 34.5900' N	45º 18.8550 'W	2177.3	5355.3	12163.5
F (8.5)	23º 33.87262' N	45º 16.65505 'W	2517.3	9101.4	12685.2

Table 2c. Transponder Net #3
This net configuration was used for ABE Dive 144,145, Jason Dives 112,113,114

ID	Latitude	Longitude	Depth (m)	X (m)	Y (m)
G (11.5)	23º 27.56755' N	45º 21.68352 'W	2777	538.9	-798.2
H (9.5)	23º 28.12634' N	45º 22.08457 'W	2556	-144.0	233.2
I (10.0)	23º 29.03513' N	45º 22.31319 'W	2129	-533.3	1910.6
J (8.5)	23º 29.13406' N	45º 20.48773 'W	2167	2575.1	2093.2

Table 2d. Transponder Net #4

This net configuration was used for ABE Dive 144,145 Jason dives 112,113,114

ID	Latitude	Longitude	Depth (m)	X (m)	Y (m)
J (8.5)	23º 29.13406' N	45º 20.48773 'W	2167.8	2575.1	2093.2
K (9.5)	23º 28.51594' N	45º 18.60549 'W	2015.0	5780.2	952.3
L (10.0)	23º 28.03803' N	45º 17.05405 'W	1997.4	8422.0	70.2
M (11.5)	23º 27.64665' N	45º 15.04713 'W	2606.3	11839.4	-652.2

Table 2e. Transponder Net #5

Net used for Jason Dive 117

	Latitude	Longitude	Depth (m)	X (m)	Y (m)
N (11)	23º 22.540' N	45º 26.218 'W	3272.9	-7182.6	-10077.5
O (11.5)	23º 23.807' N	45º 25.820 'W	3245.3	-6505.1	-7739.1

Table 3. JASON Dive Statistics

DIVE	Start/launch	Start data	End data	End/On deck		Data Duration	Lowering Duration	Max Depth
J2-110	11/20/04 22:14	11/21/04 01:01	11/21/04 02:31	11/21/04 04:12	Babel Dome Northern scarp	00 01:30:00	00 05:58:00	3006
J2-111	11/20/04 18:07	11/21/04 20:22	11/22/04 06:50	11/22/04 08:25	Babel Dome Northern scarp	00 10:28:00	01 14:18:00	2949
J2-112	11/25/04 15:04	11/25/04 17:26	11/28/04 17:43	11/28/04 19:51	Cain Dome east	03 00:17:00	03 04:47:00	2918
J2-113	11/29/04 19:38	11/29/04 21:41	12/01/04 04:01	12/01/04 05:40	Cain Dome west	01 06:20:00	01 10:02:00	2894
J2-114	12/01/04 23:00	12/02/04 00:05	12/02/04 14:33	12/02/04 16:49	Cain Dome west	00 14:28:00	00 17:49:00	2646
J2-115	12/03/04 20:36	12/03/04 21:12	12/03/04 21:29	12/03/04 22:22	Test dunk	00 00:17:00	00 01:46:00	1000
J2-116	12/04/04 15:06	12/04/04 16:50	12/06/04 01:35	12/06/04 03:03	Cain Dome crossover	01 08:45:00	01 11:57:00	2421
J2-117	12/07/04 06:00	12/07/04 08:27	12/09/04 04:18	12/09/04 06:19	Southern Scarp	01 19:51:00	02 00:19:00	3534
TOTAL					Totals:	08 13:56:00	10 18:56:00	(na)

Table 4. ABE Dive Statistics

Dive	SM2000	Chirp	Camera	Total dive duration	Survey Duration
142	04/11/19 23:16:15.8 04/11/20 09:37:15.4	04/11/19 23:16 04/11/20 09:37:44.5		13.72	6.92
143	None	04/11/23 03:59:47.5 04/11/23 09:15:48.0	04/11/22 23:39 04/11/23 00:10	19.65	13.20
144	04/11/24 14:29:41.2 04/11/25 07:47:13.3	04/11/24 17:30:28.2 04/11/25 07:00:38.6		20.17	14.51
145	04/11/28 16:37:12.3 04/11/29 10:32:47.6	04/11/28 19:37:49.7 04/11/29 10:32:39.1		22.23	14.93
146	04/12/02 13:28:44.8 04/1203 05:31:41.6	04/12/03 01:07:37.1 04/12/03 03:57:59.0	04/12/03 00:18 04/12/03 01:06	10.10	5.21
147	None	04/12/03 17:19:37.7 04/12/04 07:25:37.1		19.12	13.65
148	04/12/05 22:57:15.2 04/12/05 22:59:07.8 04/12/05 23:52:59.9 04/12/06 18:23:33.4	04/12/05 22:57:47.2 04/12/06 18:23:39.1		20.89	16.25
149	04/12/09 06:26:39.6 04/12/09 11:36:07.5	None		16.13	11.34

Table 5. Kane Megamullion KN180-2 dredge ship locations.

Pinger Over				Decimal		Latitude		Longitude		
Dr#	Date	Hour	Min	Lat	Lon	Deg.	Min.	Deg.	Min	Depth
1	324	19	48	23.5722	-45.3276	23	34.334	-45	-19.656	3040
2	325	7	51	23.5453	-45.3333	23	32.719	-45	-20.001	3054
3	325	13	1	23.5855	-45.2967	23	35.128	-45	-17.802	2586
4	325	17	34	23.5126	-45.3450	23	30.756	-45	-20.701	2487
5	326	5	50	23.4709	-45.3579	23	28.253	-45	-21.471	2832
6	326	9	50	23.5296	-45.3413	23	31.778	-45	-20.475	3017
7	326	13	57	23.4954	-45.3475	23	29.724	-45	-20.848	2623
8	327	16	13	23.5970	-45.3210	23	35.819	-45	-19.259	2887
9	327	20	19	23.6116	-45.3131	23	36.698	-45	-18.788	3380
10	328	4	44	23.5831	-45.2673	23	34.985	-45	-16.040	2630
11	328	8	12	23.5743	-45.2281	23	34.456	-45	-13.689	3144
12	328	13	22	23.6071	-45.2856	23	36.423	-45	-17.138	2651
13	329	7	59	23.4786	-45.2266	23	28.716	-45	-13.599	3587
14	329	13	59	23.4610	-45.3059	23	27.659	-45	-18.356	2557
15	329	22	34	23.4546	-45.2787	23	27.277	-45	-16.723	2663
16	330	3	8	23.4541	-45.2580	23	27.246	-45	-15.481	2913
17	333	23	17	23.4797	-45.3838	23	28.780	-45	-23.030	2496
18	334	4	28	23.4822	-45.4167	23	28.930	-45	-25.000	2980
19	334	9	25	23.5189	-45.3616	23	31.131	-45	-21.697	2732
20	336	7	10	23.3124	-45.3842	23	18.743	-45	-23.052	3646
21	336	12	5	23.3642	-45.3770	23	21.849	-45	-22.621	3112
22	336	16	41	23.4121	-45.2584	23	24.727	-45	-15.504	3406
23	338	4	35	23.4710	-45.2472	23	28.260	-45	-14.830	2960
24	338	13	2	23.4403	-45.3931	23	26.416	-45	-23.585	3432
25	339	0	11	23.3951	-45.4150	23	23.706	-45	-24.902	3440
26	341	7	38	23.4007	-45.3848	23	24.041	-45	-23.090	3385
27	341	13	46	23.4049	-45.4136	23	24.291	-45	-24.817	3584
28	344	14	24	23.3834	-45.3823	23	23.002	-45	-22.939	3280

Dredge Off-Bottom				Decimal		Latitude		Longitude		
Dr#	Date	Hour	Min	Lat	Lon	Deg.	Min.	Deg.	Min	Depth
1	325	1	49	23.5730	-45.3197	23	34.381	-45	-19.183	2454
2	325	11	18	23.5384	-45.3283	23	32.304	-45	-19.698	2426
3	325	15	2	23.5890	-45.2967	23	35.340	-45	-17.800	2480
4	325	19	56	23.5068	-45.3383	23	30.407	-45	-20.300	2374
5	326	8	22	23.4751	-45.3509	23	28.504	-45	-21.052	2457
6	326	12	32	23.5246	-45.3349	23	31.476	-45	-20.096	2612
7	326	16	20	23.4906	-45.3408	23	29.435	-45	-20.450	2355
8	327	18	52	23.5910	-45.3142	23	35.462	-45	-18.854	2331
9	327	23	36	23.6031	-45.3100	23	36.185	-45	-18.598	2790
10	328	6	47	23.5867	-45.2651	23	35.200	-45	-15.905	2463
11	328	11	48	23.5811	-45.2334	23	34.866	-45	-14.003	2778
12	328	16	15	23.5983	-45.2824	23	35.900	-45	-16.946	2421
13	329	11	10	23.4819	-45.2333	23	28.915	-45	-14.000	3179
14	329	16	45	23.4667	-45.3001	23	28.000	-45	-18.008	2197
15	330	1	30	23.4621	-45.2816	23	27.727	-45	-16.894	2313
16	330	7	30	23.4603	-45.2642	23	27.616	-45	-15.852	2575
17	334	2	14	23.4900	-45.3831	23	29.398	-45	-22.984	2293
18	334	7	24	23.4857	-44.5919	23	29.143	-45	24.485	2550
19	334	12	33	23.5139	-45.3676	23	30.832	-45	-22.058	2479
20	336	10	9	23.3126	-45.3758	23	18.758	-45	-22.546	3245
21	336	14	45	23.3613	-45.3709	23	21.676	-45	-22.253	2809
22	336	20	11	23.4218	-45.2627	23	25.309	-45	-15.761	2996
23	338	7	10	23.4752	-45.2528	23	28.509	-45	-15.165	2701
24	338	16	12	23.4468	-45.3914	23	26.807	-45	-23.485	3256
25	339	4	22	23.3932	-45.4067	23	23.593	-45	-24.402	2780
26	341	10	40	23.3980	-45.3942	23	23.881	-45	-23.654	2940
27	341	17	20	23.4052	-45.4025	23	24.315	-45	-24.152	2971
28	344	17	44	23.3834	-45.3905	23	23.003	-45	-23.427	2848

* MAPR depth refers to the depth determined by the pressure sensor on the MAPR instrument. The MAPR was usually placed on the wire 150 m above the dredge, immediately above the pinger. Dredge navigation comes from the Knorrs GPS and Seabeam centerbeam records. Water depths and positions were checked against the watchkeepers notes, where the times for pinger over (best estimate of start position on-bottom) and for dredge off-bottom were taken. Small discrepancies in position and depth between the two sets of records were ignored. Where the Seabeam system was switched off, the ships position as recorded by the watchstander on duty was used. Water depths below ship were not recorded, but can be obtained by ploting dredge positionson he Seabeam map. Where center beam depth data disagreed significantly with the watch records, the depth recorded by the watchstander was used. Date given is Julian day. No CB - depth recorder off during dredge to avoid interference with the autonomous benthic explorer (ABE).

Table 6. Kane Megamullion KN180-2 Rock sample summary (Dredge and Jason samples).

Dredge or Dive	Contents	wt. (kg)	logged	Peridotite	Dunite	Gabbro	Diabase	Basalt	% Peridotite	% Dunite	% Gabbro	% Diabase	% Basalt
1	17.4 kg pillow basalt, 1.6 kg basalt	19.0	12	0	0	0	0	19	0.0	0.0	0.0	0.0	100.0
2	8.3 kg pillow basalt +0.4 kg in bags	8.7	21					8.3	0.0	0.0	0.0	0.0	100.0
3	Empty	0.0	0										
4	37 kg peridotite, 0.1 kg dunite, 1.8 kg carbonate	38.8	3	36.7	0.1				99.7	0.3	0.0	0.0	0.0
5	64.2 kg peridotite, 3 kg gabbro, 0.1 carbonate with basalt shards	67.3	31	64.2		3			95.5	0.0	4.5	0.0	0.0
6	1.85 kg pillow basalt & hyaloclastite, 15.4 kg basalt, 2.4 kg carbonates	19.7	7					17.25	0.0	0.0	0.0	0.0	100.0
7	23.2 kg pillow basalt, 0.4 kg carbonate clasts	23.6	6					23.2	0.0	0.0	0.0	0.0	100.0
8	59.0 kg pillow basalt & hyaloclastite breccia, 32.6 kg basalt, 0.3 kg coral	91.9	31					91.6	0.0	0.0	0.0	0.0	100.0
9	16.5 kg gabbro, 22.5 kg basalt and basalt breccia, 27.0 kg pillow basalt and pillow basalt breccia, 5.2 kg polymict breccia, 6.2 kg diabase	77.4	39					91.6	0.0	0.0	0.0	0.0	100.0
10	Empty	0.0	0										
11	57.7 kg gabbro, 10.1 kg pillow basalt and palagonite breccia, 0.7 kg soapstone & peridotite, 2.8 kg gravel & mudstone	71.8	7	0.7		57.7		10.1	1.0	0.0	84.2	0.0	14.7
12	3.9 kg harzburgite & soapstone, 2.6 kg gabbro, and a few bits of coral	6.5	16	3.9		2.6			60.0	0.0	40.0	0.0	0.0
13	19.1 kg diabase, 1.9 kg gabbro, 2 kg pillow basalt & 1.9 kg basalt, 8 kg polymict cataclastic breccia, 0.1 kg lithified chalky ooze, 1.6 kg pebbles	37.3	56			1.9	19.1	3.9	0.0	0.0	7.6	76.7	15.7
14	99.4 kg harzburgite, 13.4 kg gabbro, 16.4 kg pillow basalt, 1.7 kg basalt, 7.2 kg diabase, 0.3 polymict breccia, 9.8 kg gravel	148.2	71	99.4		13.4	7.2	18.1	72.0	0.0	9.7	5.2	13.1
15	13.2 kg harzburgite, 28 kg diabase, 1.9 kg gabbro, 1.4 kg carbonate.	44.5	41	13.2		1.9	28		30.6	0.0	4.4	65.0	0.0
16	7.9 kg pillow basalt, 0.2 kg basalt, 0.2 kg diabase, 0.1 kg soapstone, 3.2 kg Fe-Mg crusts, 12.6 kg oolitic chalk, 0.1 kg coal slag.	24.3	28	0.1			0.2	8.1	1.2	0.0	0.0	2.4	96.4
17	33 kg harzburgite, 0.3 kg coral, 1.4 kg assorted pebbles.	35.0	18	33					100.0	0.0	0.0	0.0	0.0
18	26.7 kg pillow basalt, 7.1 kg basalt, 4 kg diabase, 1.5 kg gabbro, 1.5 kg dunite, 24.4 kg harzburgite, and 6 kg pebbles.	70.6	42	24.4	1	1.5	4	33.8	37.7	1.5	2.3	6.2	52.2
19	1.6 kg gabbro, 34.9 kg harzburgite, 2.2 kg marlstone, 4.6 kg carbonates, 14.8 kg pebbles	58.1	49	34.9		1.6			95.6	0.0	4.4	0.0	0.0
20	34 kg pillow basalt, 97.8 kg basalt.	131.8	40					131.8	0.0	0.0	0.0	0.0	100.0

21	0.1 kg basalt, 1.8 kg diabase, 10.5 kg gabbro, 4.7 kg dunite, 18.6 kg harzburgite, 0.7 kg Marlstone, 7 kg pebbles.	43.4	32	18.6	4.7	10.5	1.8	0.1	52.1	13.2	29.4	5.0	0.3
22	46 kg basalt	46.0	2					46	0.0	0.0	0.0	0.0	100.0
23	Empty	0.0	0										
24	2.7 kg peridotite, 0.05 kg metagabbro	2.7	12	2.7		0.05			98.2	0.0	1.8	0.0	0.0
25	0.15 pillow basalt, 0.1 kg basalt, 4.9 kg diabase, 24.9 kg gabbro.	30.2	30			24.9	4.9	0.25	0.0	0.0	82.9	16.3	0.8
26	10.3 kg pillow basalt, 30.5 kg basalt, 7.3 kg diabase, 10.3 kg gravel.	56.6	20				4.9	40.8	0.0	0.0	0.0	10.7	89.3
27	2.5 kg pillow basalt, 0.5 kg basalt, 64.8 kg gabbro, 31.6 dunite, 17.7 kg harzburgite, 136.7 kg gravel.	253.8	103	17.7	31.6	64.8		3	15.1	27.0	55.3	0.0	2.6
28	3.3 kg gabbro, 1 kg dunite, 24.7 kg harzburgite & lherzolite, 5.5 kg marlstone, 17 kg pebbles.	51.5	39	24.7	1	3.3			85.2	3.4	11.4	0.0	0.0
28	*Total for Dredges*	*1458.7*	*756.0*	*374.2*	*38.4*	*187.2*	*70.1*	*546.9*	*30.8*	*3.2*	*15.4*	*5.8*	*44.9*
Jas 110	26.8 kg basalt	26.8	8					26.8	0.0	0.0	0.0	0.0	100.0
Jas 111	47.6 kg pillow basalt, 33.1 kg basalt, 0.2 kg coral	80.9	21					80.7	0.0	0.0	0.0	0.0	100.0
Jas 112	13.5 kg pillow basalt, 3 kg diabase, 34.9 gabbro, 3.6 kg dunite, 308.9 kg peridotite, 42.05 kg marlstone.	405.9	119	308.9	3.6	34.9	3	13.5	84.9	1.0	9.6	0.8	3.7
Jas 113	5.5 kg diabase, 42.9 gabbro, 1.8 dunite, 165.8 kg peridotite, .9 kg marlstone	217	73	165.8	1.8	42.9	5.5		76.8	0.8	19.9	2.5	0.0
Jas 114	53.8 kg pillow basalt, 24.4 kg gabbro, 4.6 kg dunite, 130 kg peridotite, 1.6 kg other	214.4	24	130	4.6	24.4		53.8	61.1	2.2	11.5	0.0	25.3
Jas 116	14.4 kg pillow basalt, 48.3 basalt, 10.6 diabase, 7.6 gabbro, 15.4 peridotite, 7.3 hydrothermal Mn	103.6	52	15.4		7.6	10.6	62.7	16.0	0.0	7.9	11.0	65.1
Jas 117	11.2 pillow basalt, 16.4 basalt, 52.7 diabase, 75 gabbro, 3.1 marl.	158.4	89			75	52.7	27.6	0.0	0.0	48.3	33.9	17.8
7	*Total for Jason Dives*	*1207*	*386*	*620.1*	*10*	*184.8*	*71.8*	*265.1*	*238.727*	*3.984*	*97.1*	*48.31*	*312*
35	*All Samples*	*2665.7*	*1142*	*994.3*	*48.4*	*372.0*	*141.9*	*812.0*	*42.0*	*2.0*	*15.7*	*6.0*	*34.3*

Table 7. Jason Instrument Locations

Jason Instrument Locations				
Origin				Located on the deck line, center front of the vehicle.
Reference Frame	**x**	**y**	**z**	
	Positive	Positive to	Positive	
	forward	stbd	down	
Instrument	**x (cm)**	**y (cm)**	**z (cm)**	**Comment**
1st configuration				Dives J2-110 through J2-112
Imagenex	0	39	-241	Mid-point of the instrument
SM2000	4	0	-227.5	Mid-point of the plate of the instrument (horizontal in this configuration)
Magnetometer	-8.5	-99	-235	Top of the instrument
Still Camera	10	0	-237.5	Center of the lens (oriented horizontal, forward facing)
Brow Camera	9	23.5	-211.5	Center of the lens
Pilot P/T	-11	-19.5	-121	Center of the lens
Science P/T	-9	40	-106.5	Center of the lens
2nd configuration				Dives J2-113 to end of cruise
SM2000	-281.94	0	-76.2	Mid-point of the plate of the instrument (vertical in this configuration)
Still Camera				Re-oriented to 47° from horizontal